MISSOURI S&T
Library and
Learning Resources

Scholars' Mine

Doctoral Dissertations

Student Theses and Dissertations

Summer 2010

Ultracapacitor character analysis and its application in unified power quality conditioner as energy storage system

Xiaomeng Li

Follow this and additional works at: https://scholarsmine.mst.edu/doctoral_dissertations

Part of the Electrical and Computer Engineering Commons

Department: Electrical and Computer Engineering

Recommended Citation

Li, Xiaomeng, "Ultracapacitor character analysis and its application in unified power quality conditioner as energy storage system" (2010). *Doctoral Dissertations*. 1905.
https://scholarsmine.mst.edu/doctoral_dissertations/1905

ULTRACAPACITOR CHARACTER ANALYSIS AND ITS APPLICATION IN

UNIFIED POWER QUALITY CONDITIONER AS ENERGY STORAGE SYSTEM

by

XIAOMENG LI

A DISSERTATION

Presented to the Faculty of the Graduate School of the

MISSOURI UNIVERSITY OF SCIENCE and TECHNOLOGY

In Partial Fulfillment of the Requirements for the Degree

DOCTOR OF PHILOSOPHY

in

ELECTRICAL ENGINEERING

2010

Approved by

Dr. Mariesa L. Crow, Advisor
Dr. Badrul H. Chowdhury
Dr. Mehdi Ferdowsi
Dr. Bruce M. McMillin

PUBLICATION DISSERTATION OPTION

This dissertation consists of the following three articles that have been submitted for publication as follows:

Paper 1: X. Li, M. L. Crow, "Ultracapacitor Frequency Analysis and its Equivalent Circuit Modeling", accepted by the Proceedings of the 2009 North America Power Symposium.

Paper 2: X. Li, M. L. Crow and S. Atcitty, "Improved Performance of a Unified Power Quality Conditioner with Ultra capacitors", to be submitted to IET Journal of Electric Power Applications.

Paper 3: X. Li, M. L. Crow, "UPQC with Energy Storage System performance comparison by using PI and H∞ method", to be submitted to the Proceedings of the 2010 North America Power Symposium.

ABSTRACT

This dissertation focuses on the Ultracapacitor (UCAP) character analysis and its application in Unified Power Quality Conditioner (UPQC) as an Energy Storage System (ESS) for improved UPQC performance. It includes three parts as described below.

The first part is Paper I. The UCAP is a popular choice for the ESS because of its distinct characters. In the application UCAP's transient behavior need to be studied for design purpose. Usually these transient characters are not shown in the product data sheet. In this paper UCAP frequency analysis is performed, and based on the test data the equivalent model of the UCAP is built. The fitting result shows that using multi-level ladder circuit can perfectly fit the UCAP transient characters.

The second part is Paper II. A UPQC is to compensate both source voltage sag and load current imperfections in power distribution system. With the UCAP based Energy Storage System, the UPQC has an optimized power flow between UPQC and system during the transit state, also the UPQC's serial and shunt part has an improved performance with UCAP. The impact of UCAP model on its control and simulation is analyzed. From the analysis, UCAP based Energy Storage System can well fulfill the requirement of UPQC to provide high active power during transit time and improve the UPQC overall performance.

The third part is Paper III. Conventionally the PI control method is applied in UPQC, including DVR and APF part. With ESS the H∞ control method is applied in UPQC. This paper shows that the two methods have their own advantages and disadvantages. In the practical application the control method can be chosen by considering the different transit states.

ACKNOWLEDGMENTS

First of all, I would like to extend my gratitude to Dr. Mariesa L. Crow for sparking my interest in the areas of power quality and distribution power device area when I took her class at the beginning of my PhD program. And many thanks to her for offering me many rewarding research opportunities over the years and educating me not only in a full set of engineering skills, but also the systematic methodology to initiate and carry out researches.

I wish to thank Dr. Mehdi Ferdowsi for his guidance in the exciting world of power electronics, which became an integral part of this dissertation research. I'm also in debt to research advices from Dr. Keith Corzine. The help from Dr. Badrul Chowdhury and Dr. Bruce McMillin are very much appreciated.

Special thanks to Jerry Tichenor for his help in building the hardware testing platform. Over the years, the cooperation from my colleagues in Power Group: Keyou Wang, Lisheng Shi, Theresa Odun-Ayo and Fanjun Meng, is very important for many research successes.

Endless thanks go to my dear Mom and Dad for their constant support and love. Making them proud of me is the most important motivation for my pursuit of a PhD degree.

TABLE OF CONTENTS

LIST OF ILLUSTRATIONS

LIST OF TABLES

DISSERTATION INTRODUCTION

Power quality is a very important issue in the presence of sensitive loads such as digital electronics, communication systems, and manufacturing processes. The Unified Power Quality Conditioner (UPQC) is a distribution-level controller which is to compensate both source voltage sag and load current imperfections in power distribution system. Recently the Energy Storage System (ESS) is widely applied in power electronics devices. Despite the variety of the energy storage devices, the Ultracapacitor (UCAP) or so-called electrochemical capacitor is one of the most popular choices for the energy storage system because of its distinct characters. This dissertation focuses on the UCAP character analysis and its application in UPQC as an ESS for improved UPQC performance. It is organized in three parts as described below.

The first part is Paper I. It deals with the UCAP characters analysis. UCAP is a relatively new device in the energy storage area which offers high power density and extremely high cycling capability. Recent developments in basic technology have made UCAP an interesting option for short-term energy storage in power electronic system. Using a UCAP based energy storage system can increase the power electronics system design flexibility, leading to a system with better performance, lower costs, and physically smaller in size and weight. The UCAP or called electrochemical capacitors are of two types: one is double-layer capacitor which has high specific area carbon materials interracially, and the other is pseudo capacitor, which associated with electrosoption and surface redox processes.

In order to optimize the UCAP application and realize its advantages, detailed performance information is needed for the UCAP. This information is usually unavailable

from product data sheets. They usually include major important parameters like capacity and series resistance with several constant-current discharge curves, but little or no transient response information in the data sheets. UCAP model is critically important for design purposes, because different models of UCAP can lead to varying degrees of accuracy in simulation and control development. Hardware experiments using frequency analysis is applied for the UCAP module, and UCAP transient behavior data were got from the test. Based on the test data, the different order levels equivalent Ladder Circuit models for the UCAP are built up using Least Square Fitting method. Results show that with higher order, the Ladder Circuit fitting method becomes more accurate. With this equivalent model, the UCAP can be easily combined with various application environments so that to find analytical or numerical solutions.

The second part is Paper II. It shows the UPQC performance improvement with UCAP based ESS. With the increase of the complexion in the power distribution system, it is very possible that several kinds of power quality disturbances are happened in a power distribution system simultaneously. Loads such as diode converters produce large harmonics interferences. Voltage disturbance is also a big problem for sensitive consumers. In order to improve the reliability and efficiency of power distribution system, it is important to introduce UPQC as a distribution-level controller for Power Quality. UPQC is usually installed at the point of common coupling of industry loads. The UPQC consists of two voltage source inverters (VSI) connected back to back sharing a common DC-link. One inverter acts as a serial dynamic voltage regulator (DVR) whereas the other acts as a shunt active power filter (APF). The purpose of the serial DVR is to insulate the load against any sags or swells from the source. The purpose of the shunt

APF is to filter the harmonic content of the load to keep the source side current clean. Conventionally the DC-link voltage is maintained by the shunt APF exchanging active power with the system. Recently the ESS such as UCAP is applied into the UPQC DC-link, which can provide high pulse power during transit states.

UCAP are electrical energy storage devices which offer high power density and high cycling capability. It can be used as a rapid discharge energy storage for power applications. UCAP has been used extensively in pulsed power applications for high-energy physics and weapons applications. Ideal power system applications for UCAP are short duration storage applications such as power stabilization, power quality ride-through applications, and voltage flicker mitigation among other applications that require high power density and rapid recharge. The major difference between an UCAP compared to a conventional capacitor is that the liquid electrolyte structure and porous electrodes give the UCAP a high effective area that minimizes the distance between the two plates. Additionally, UCAP has cells that can be connected in serial and parallel to obtain the desired voltage level and capacitance. By utilizing a bidirectional DC/DC converter, the UCAP is an attractive solution for UPQC to provide large amounts of short term active power. The DC/DC converter operates to alternate between boost, buck, and idle modes. By this way the bidirectional power flow is realized between UCAP and UPQC to fulfill the UPQC active power requirement.

With UCAP the UPQC has an optimized power flow between UPQC and system during the transit state. Also the UPQC's DVR and APF part has an improved performance with UCAP. Furthermore, the UCAP character is experimentally analyzed and its equivalent circuit model is built. The impact of UCAP model on its control and

simulation is analyzed. From the analysis, UCAP based Energy Storage System can well fulfill the requirement of UPQC to provide high active power during transit time, and improve the UPQC overall performance.

The third part is Paper III. It shows the new H∞ control method applied into UPQC with ESS and its comparison with conventional PI control method. Multiple power quality regulation functions are implemented in UPQC simultaneously with a high performance ratio. Conventionally the PI control method is applied in UPQC control scheme, including DVR and APF part. Recently the H∞ control method is widely applied in Power Quality area. This paper shows the control schemes of PI and H∞ method in UPQC, and their performance is compared under different conditions. The simulation results show that the two methods have their own advantages and disadvantages. If the regular load is changed frequently, H∞ method has better performance. If harmonic load is changed frequently, PI method is better. In the practical application the control method can be chosen by considering the different transit states.

PAPER I

Ultracapacitor Frequency Analysis and its Equivalent Circuit Modeling

Xiaomeng Li, Mariesa L. Crow
Electrical and Computer Engineering
Missouri University of Science and Technology
Rolla, MO 65409

ABSTRACT

Energy storage system is becoming more and more important in power electronics device. The Ultracapacitor or so-called electrochemical capacitor is one of the most popular choices for the energy storage system because of its distinct characters. In the application UCAP's transient behavior need to be studied for design purpose. Usually these transient characters are not shown in the product data sheet. In this paper UCAP frequency analysis is performed, and based on the test data the equivalent model of the UCAP is built. The fitting result shows that using multi-level ladder circuit can perfectly fit the UCAP transient characters.

Keywords

Ultracapacitor, Frequency Analysis, Ladder Circuit.

I. INTRODUCTION

The newly available technology of ultracapacitor (UCAP) is making it easier for engineers to balance their use of both energy and power. UCAP is a relatively new device in the energy storage area which offers high power density and extremely high cycling capability [1]-[3]. Recent developments in basic technology have made UCAP an interesting option for short-term energy storage in power electronic system. Using a UCAP based energy storage system can increase the power electronics system design flexibility, leading to a system with better performance, lower costs, and physically smaller in size and weight. The UCAP or called electrochemical capacitors are of two types [4]: one is double-layer capacitor which has high specific area carbon materials interracially, and the other is pseudo capacitor, which associated with electrosoption and surface redox processes.

In order to optimize the UCAP application and realize its advantages, detailed performance information is needed for the UCAP. This information is usually unavailable from product data sheets. They usually include major important parameters like capacity and series resistance with several constant-current discharge curves [5]-[7], but little or no transient response information in the data sheets. Transient behavior is critically important for design purposes, because many applications are used where UCAP has power variations from the average state. With the test data got from frequency analysis, equivalent circuit model of UCAP is built up to follow its transient behavior. The fitting result shows that using multi-level ladder circuit can perfectly fit the UCAP transient behavior.

II. BASIC CHARACTERS OF UCAP

Normally capacitors store electric energy by accumulating positive and negative charges (often on parallel plates) separated by an insulating dielectric [8]. The capacitance, C, represents the relationship between the stored charge, q, and the voltage between the plates, V, as shown in (1). The capacitance depends on the permittivity of the dielectric, ε , the area of the plates, A, and the distance between the plates, d, as shown in (2). Equation (3) shows that the energy stored on the capacitor depends on the capacitance and on the square of the voltage.

$$q = CV \tag{1}$$

$$C = \frac{\varepsilon A}{d} \tag{2}$$

$$E = \frac{1}{2}CV^2 \tag{3}$$

The amount of energy a capacitor is capable of storing can be increased by either increasing the capacitance or the voltage stored on the capacitor. The stored voltage is limited by the voltage-withstand-strength of the dielectric (which impacts the distance between the plates). Capacitance can be increased by increasing the area of the plates, increasing the permittivity, or decreasing the distance between the plates.

Ultracapacitors are available in a variety of sizes and configurations. They are designed to satisfy the most important requirements of power sources: To provide bursts of power in the seconds range over many hundreds of thousands of cycles.

The UCAP module studied in this paper is a product by ESMA Company [9]. The module number is 30EC402-220-42/21-0.009. The detail company specifications are shown in Table 1. It shows some typical data of normal UCAP.

Compared with other energy storage device such as battery [10], [11], The UCAP has better discharge cycle life, efficiency, lifetime, response time, and easier maintenance.

The charge or discharge curve can be used to test UCAP module profile values. Figure1 is a discharging curve for a given load resistance. Ch1 is voltage magnitude and Ch2 is current magnitude. The discharging curve shows that in the UCAP operating voltage window the UCAP works exactly like a normal capacitor, except big capacitance.
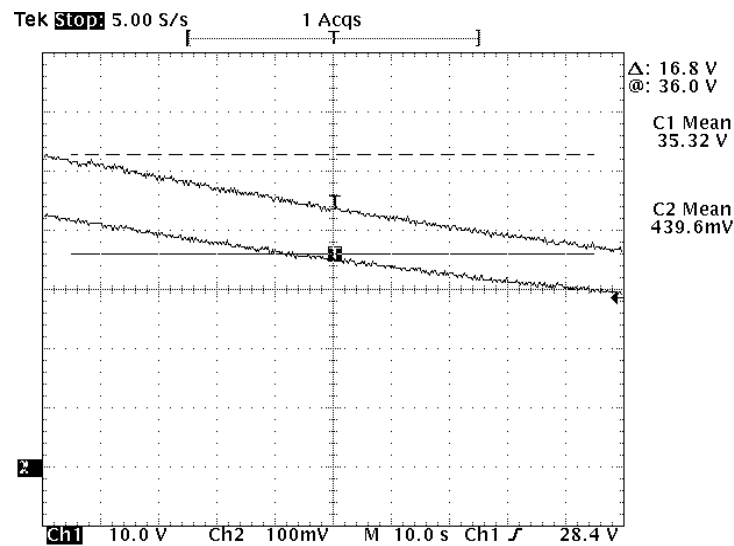
Fig. 1 Discharge curve of the UCAP module 30EC402

Table 1. 30EC402 U Capacitor Module datasheet

Operating voltage window, V	45~12
Maximum voltage, V (at this voltage for only a short period)	48
Minimum voltage, V	12
Internal Ohmic resistance, $m\Omega + 25^oC(-30^oC)$	9 (12)
Capacitance, F	330
Energy stored within operating voltage window, kJ	310
Energy stored within 42-12 V voltage window, kJ	270
Maximum power, kW	56
Leakage current at 42 V, mA	15
Overall dimensions, mm (L*W*H)	530*180*262
Weight, kg	40
Operating temperature, ^oC	-50/+50
Storage temperature, ^oC	-60/+70
Cycle life, cycles	$3*10^5$

III. FREQUENCY ANALYSIS OF UCAP

Frequency analysis is a method to measure the complex impedance of the UCAP module [12]. When the UCAP is being discharged, adding some AC components in the discharging current. The AC component is in certain frequency range. By testing the current and response AC voltage, we can get the UCAP's frequency analysis plot. The hardware setup of the frequency analysis is shown in Figure 2.
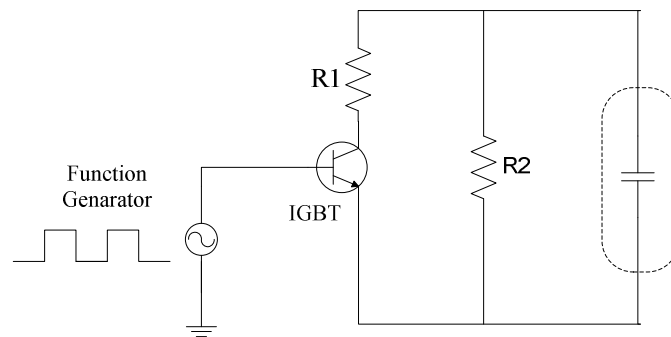
Fig. 2 Hardware setup of the UCAP frequency analysis

In the hardware setup, R1 and R2 can be adjusted to provide a desired current level. A signal generator (from NF 5060A) supplies the required drive signal to the IGBT through a standard gate drive circuit.

The charging AC current and voltage are shown in Figure 3. Ch1 is voltage and Ch2 is current. We can see that with very big current variation the voltage variation is still very small. So only the signal generator power output is not big enough for so big current and power switch (IGBT) is needed for the charging circuit.
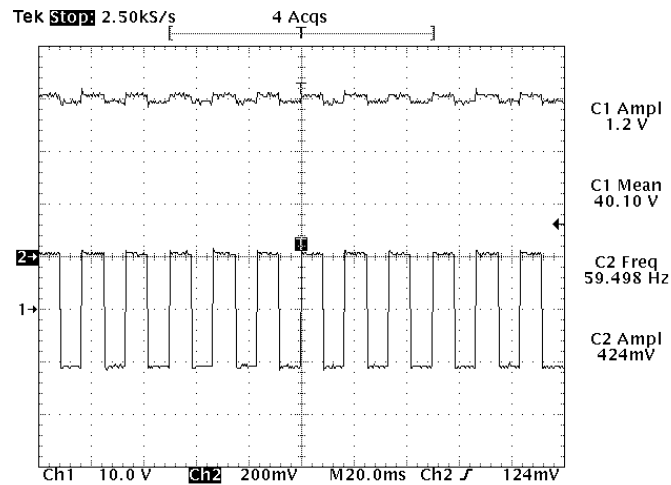
Fig. 3 Testing current and voltage for the UCAP module

The device using for test is NF 5060A Frequency Response Analyzer. It uses a frequency swept square wave to measure the gain and phase response with respect to frequency of the UCAP. The measurement frequency range is 0.001Hz to 10,000Hz. It consists of synthesized sweep oscillator which outputs the signal that drives the device under test and two input analysis channels which analyze the gain and phase response of the device under test with respect to the applied drive signal.

The analyzing software is Venable software system. The Venable system with supported Frequency Response Analyzer is a combined frequency response modeling and measurement system. The hardware portion of Frequency Response Analyzer (NF 5060A) makes measurements of gain, phase, and voltage versus frequency by coupling the analyzer to the UCAP. The software portion runs on any personal computer. Data can be saved or plotted in graphs. Graphs types supported are voltage vs. frequency (log-log),

gain and phase vs. frequency (semi-log), and reactance vs. frequency (log-log with lines for constant capacitance and inductance).

Figure 4 is a bode plot generated in Venable. The frequency range is 0.001Hz – 10,000Hz. The red one is for impedance and blue one is for phase. These frequency analysis data can also be used for UCAP equivalent circuit design.

At very low frequency, the measurement time is very long and the measurement process is very easily disturbed, so at the point near 0.001Hz the curve is not very smooth.

The Venable system can also generate a Nyquist plot shown in Figure 5.
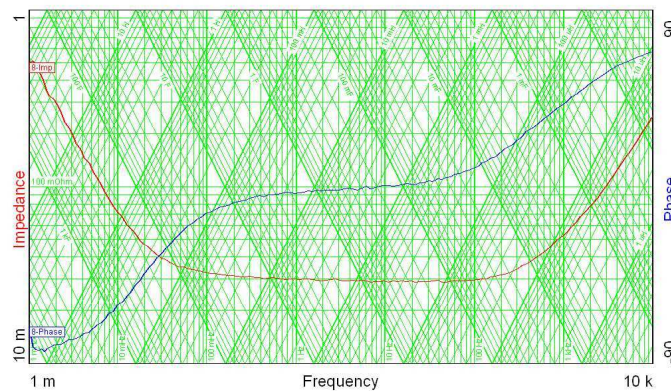
Fig. 4 Bode plot of UCAP module frequency analysis in Venable

The magnitude is plotted as radius in dB outside of the unity gain circle, which is colored black, and linearly inside the unity gain circle. This type of display allows all the data to be displayed while retaining the advantages of a standard Nyquist plot.
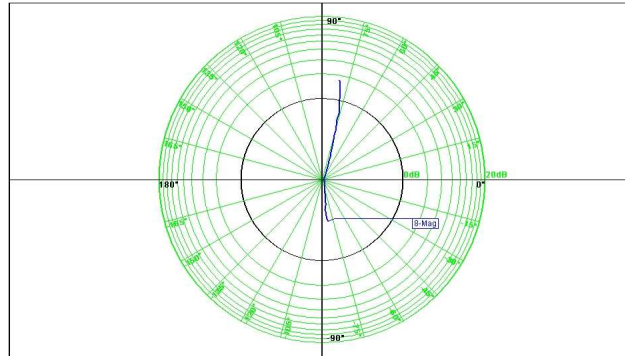
Fig. 5 Nyquist plot of UCAP module frequency analysis in Venable

If the frequency analysis data is plotted in MATLAB, the bode plot is shown in Figure 6. The black one is for real part of resistance, the blue one is for image part of resistance. From the figure the resonant frequency of the UCAP module is around 10Hz.

The standard Nyquist plot in MATLAB is shown in Figure 7.

Figure 7 is the whole frequency range of Nyquist plot. Normally the UCAP is applied in the power electronic system which typical frequency range is 0.1Hz – 500Hz. So for the equivalent circuit fitting design we only need the normal frequency range (0.1Hz – 500Hz) of the Nyquist plot, shown inside the circle. The enlarged circle area is shown in Figure 8. Since the order of the original data is very small, the data set is multiply 10^6 for the plot.
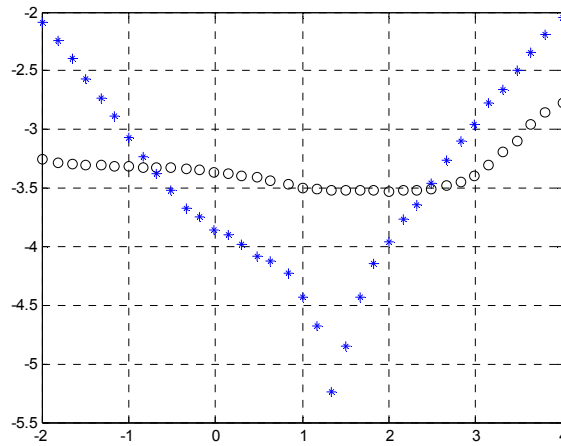
Fig. 6 Bode plot of UCAP module frequency analysis in MATLAB
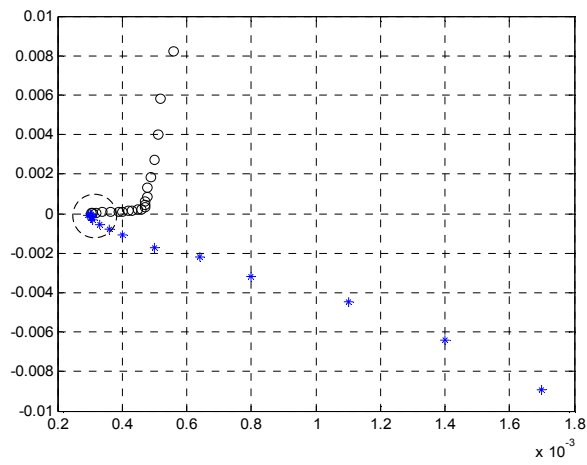
Fig. 7 Nyquist plot of UCAP module frequency analysis in MATLAB
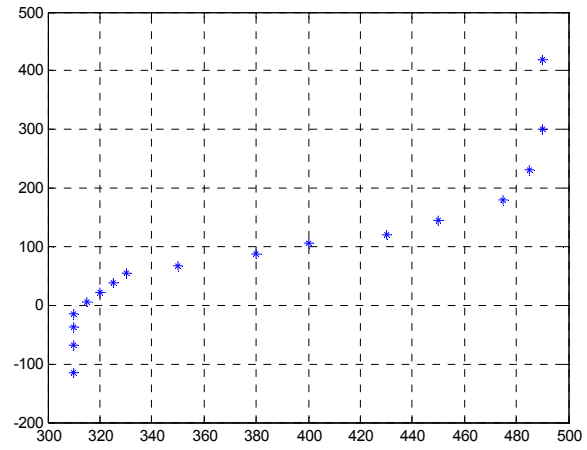
Fig. 8 Nyquist plot of UCAP module in 0.1Hz – 500Hz

IV. UCAP EQUIVALENT CIRCUIT DESIGN

A. Nonlinear Least Square Fitting Method

In general a set of N measurements can be simulated with a function of the independent variable, and a set of adjustable parameters. The form of this function depends on the physical model used to explain the measurement set. As the data set will contain random and systematic errors, it can not be reproduced exactly by the simulation function. The best fit of this function is found through minimizing the sum of the weighted squares of the difference between the measured and the simulated data sets [13].

The set of measured quantities can be denoted by the vector z which may include measurements of system states or quantities that are functions of system states:

$$z^{true} = Ax \tag{4}$$

Where x is the set of system states and A is usually not square. The error vector is the difference between the measured quantities z and the true quantities:

$$e = z - z^{true} = z - Ax \tag{5}$$

Typically the minimum of the square of the error is desired to negate any effects of sign differences between the measured and true values. So a state estimator endeavors to find the minimum of the squared error, or a least squares minimization:

$$\|e\|^2 = e^T \cdot e = \sum_{i=1}^{m} \left[z_i - \sum_{j=1}^{m} a_{ij} x_j \right]^2 \tag{6}$$

The squared error function can be denoted by U(x):

$$U(x) = e^T \cdot e = (z - Ax)^T (z - Ax)$$
$$= z^T z - z^T Ax - x^T A^T x + x^T A^T Ax$$

(7)

Note that the product $z^T Ax$ is a scalar and so it can be equivalently written as $x^T A^T z$. Therefore the squared error function is given by:

$$U(x) = z^T z - 2x^T A^T x + x^T A^T Ax$$

(8)

The minimum of the squared error function can be found by an unconstrained optimization where the derivative of the function with respect to the states x is set to zero:

$$\frac{\partial U(x)}{\partial x} = 0 = -2A^T z + 2A^T Ax$$

(9)

Thus: $A^T Ax = A^T z$

So if $b = A^T z$ and $\hat{A} = A^T A$, then $\hat{A}x = b$

Which can be solved by LU factorization. This state vector x is the best estimate (in the squared error) to the system operating condition from which the measurements z were taken. The measurement error is given by:

$$e = z^{meas} - Ax$$

(10)

We will use MATLAB for the nonlinear least square fitting design, the function in MATLAB is "lsqnonlin".

B. Classical Equivalent Circuit Designs

Because of its complex physical nature, the UCAP is best described by a distributed parameter system. The most common UCAP model is the classical equivalent circuit shown in Figure 9 [14]. It consists of a capacitance C, an equivalent series

resistance (ESR), and an equivalent parallel resistance (EPR). The ESR is a loss term that models internal heating in the capacitor and is therefore of most importance during charging and discharging. It will also reduce terminal voltage during discharge into a small load resistance due to the resistive divider effect. The EPR models the leakage effect and will therefore impact long term energy storage performances.
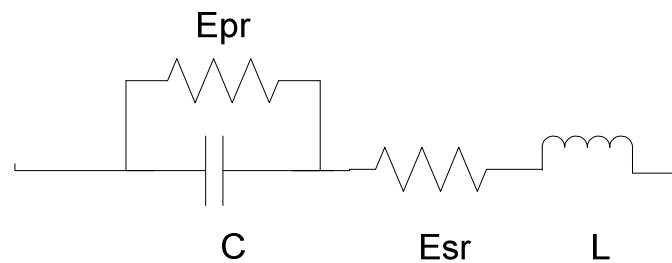
Fig. 9 Classical equivalent circuit of UCAP

C. Ladder Circuit Design

The distributed nature of the UCAP can be modeled by the ladder circuit. The ladder circuits are formed by adding RC circuit branches to the classical equivalent circuit, as shown in Figure 10. The ladder circuit provides an excellent fit to the experiment data. So the ladder circuit model can physically mimic the distributed nature of the resistance and the charge stored in a porous electrode. With this equivalent model, the UCAP can be easily combined with various loads or models so that to find analytical or numerical solutions. A simplified 1st equivalent circuit of the EC indicates parameters of most engineering interest. 2nd, 3rd, 4th order circuit will be used for fitting design.

The data file generated from frequency analysis will be used for UCAP's equivalent circuit design.
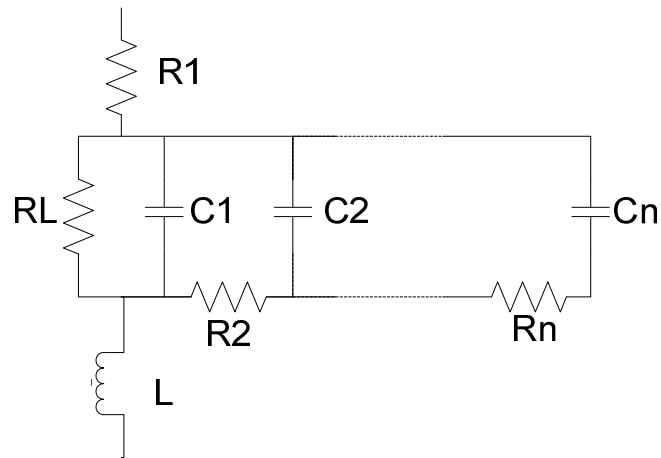
Fig. 10 Ladder circuit design of UCAP

V. RESULTS OF EQUIVALENT CIRCUIT DESIGN

Based on the Classical Equivalent Circuit model and Ladder Circuit model discussed above, the Nonlinear Least Square Fitting method is applied for each model in MATLAB.

Figure 11 is the classical equivalent circuit result after using Least Square Fitting Method. Data shown by '*' is the original experiment data. We can see that the fitting result is poor. This means this low order equivalent circuit can not show the dynamic feature of the UCAP module.

Figure 12 is the Ladder Circuit Model result after using the Least Square Fitting Method. 2nd, 3rd, 4th order circuits are shown respectively. Detail equivalent circuit parameters are also shown below with each residual norm.
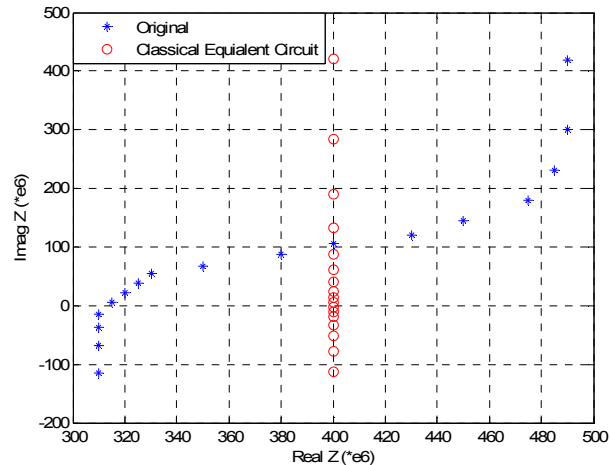
Fig. 11 Classical Equivalent Circuit Model for the UCAP
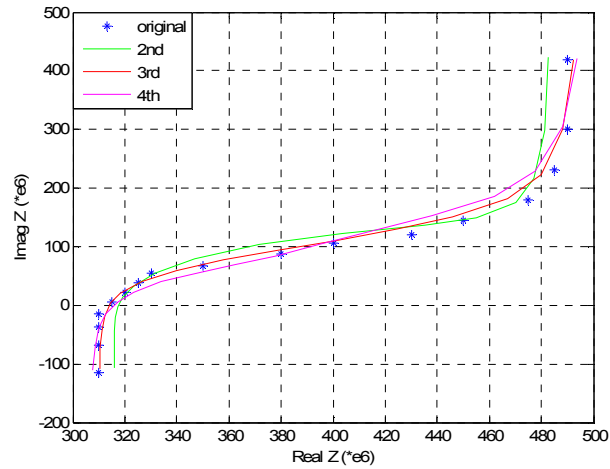
Fig. 12 Ladder Circuit Model for UCAP

From Table 2 we can find that with Ladder Circuit's order increases, the residual

norm of the Least Square Fitting method decreases. This means that higher order Ladder

Circuit model can fit the transient behavior of the UCAP module much better.

Table 2. Ladder Circuits parameters and their residual norm

	L (*e-6H)	R1 (*e-6Ω)	C1 (*e6F)	R2 (*e-6Ω)	C2 (*e6F)	R3 (*e-6Ω)	C3 (*e6F)	R4 (*e-6Ω)	C4 (*e6F)	residue norm (*e-6)
2nd	0.1771	315.69	0.00035	255.88	0.00151					44.52
3rd	0.1837	310.18	0.00027	172.44	0.00077	279.87	0.00088			29.06
4th	0.1876	307.74	0.00023	130.22	0.00044	157.65	0.0007	291.73	0.00055	27.76

VI. CONCLUSIONS

UCAP becomes an important device as energy storage system in the power electronic system. Usually the UCAP factory datasheet only contains parameters like capacity and series resistance with several constant-current discharge curves, where little or no transient response information included. Hardware experiments using frequency analysis is applied for the UCAP module, and UCAP transient behavior data were got from the test. Based on the test data, the different order levels equivalent Ladder Circuit models for the UCAP are built up using Least Square Fitting method. Results show that with higher order, the Ladder Circuit fitting method becomes more accurate. With this equivalent model, the UCAP can be easily combined with various application enviroments so that to find analytical or numerical solutions.

VII. REFERENCES

1. A.F. Burke, J.E. Hardin, and E.J. Dowgiallo, "Application of Ultracapacitors in Electric Vehicle Propulsion Systems," Proc. 34 Int. Power Sources Symposium, Cherryhill NJ (1990).

2. J.R. Miller, "Battery-Capacitor Power Source for Digital Communication-Simulations Using Advanced Electrochemical Capacitors," PV95-29, pp 246-254, The Electrochemical Society Proceedings Series, Pennington, NJ (1996).

3. B.E. Conway, "Electrochemical supercapacitors: scientific fundamentals and technological applications," Kluwer/Plenum, NY (1999).

4. B.E. Conway, W.G. Pell, "Double-layer and pseudocapacitance types of electrochemical capacitors and their applications to the development of hybrid devices," Vol. 7, pp 637-644, J Solid State Electrochem (2003).

5. R. Bonert, L. Zubieta, "Measurement techniques for the evalution of double-layer power capacitors," Conference Record of the 1997 Industry Applications 32nd Annual Meeting, pp 1097-1100, Oct. 1997.

6. E. Schempp and W. D. Jackson, "Systems considerations in capacitive energy storage," in Proc. 31st Intersociety Energy Conversion Engineering Conf., vol. 2, Aug. 1996, pp. 666–671.

7. G. L. Bullard, H. B. Sierra-Alcazar, H. L. Lee, and J. L. Morris, "Operating principles of the ultracapacitor," IEEE Trans. Magn., vol. 25, pp. 102–106, Jan. 1989.

8. W. V. Hassenzahl, Capacitors for Electric Utility Energy Storage: Electric Power Res. Inst., 1997, vol. WO-8812.

9. ESMA Company, http://www.esma-cap.com/.

10. J. McDowall, "Conventional battery technologies—Present and future," in Proc. 2000 IEEE Power Engineering Society Summer Meeting, vol. 3, July 2000, pp. 1538–1540.

11. M. A. Casacca, M. R. Capobianco, and Z. M. Salameh, "Lead-acid battery storage configurations for improved available capacity," IEEE Trans. Energy Conversion, vol. 11, pp. 139–145, Mar. 1996.

12. S. Buller, E. Karden, D. Kok, and R.W. De Doncker, "Modeling the Dynamic Behavior of Supercapacitors Using Impedance Spectroscopy," IEEE on Industry Application, Vol. 38, NO. 6. pp 1622-1626.

13. B.A. Boukamp, "A nonlinear least squares fit procedure for analysis of immittance data of electrochemical systems," Solid State Ionics (1986).

14. L. Zubieta, R. Robert, "Characterization of double-layer capacitors (DLC) for power electronics applications," Conference Record of the 1998 Industry Application Society 33rd Annual Meeting, Oct. 1998.

Paper II

Improved Performance of a Unified Power Quality Conditioner with Ultracapacitors

X. Li[1], M. L. Crow[1], and S. Atcitty[2]

1. Missouri University of Science and Technology, Rolla, MO 65409
2. Sandia National Laboratories, Albuquerque, NM

ABSTRACT

The object of Unified Power Quality Conditioner (UPQC) is to compensate both source voltage sag and load current imperfections in power distribution system. This paper presents an analysis of the UPQC with Ultracapacitors (UCAP). With the UCAP based Energy Storage System, the UPQC has an optimized power flow between UPQC and system during the transit state, also the UPQC's serial and shunt part has an improved performance with UCAP. The UCAP character is experimentally analyzed and its equivalent circuit model is built. The impact of UCAP model on its control and simulation is analyzed. The UPQC compensation limit with selected UCAP size is also analyzed. From the results, UCAP based Energy Storage System can well fulfill the requirement of UPQC to provide high active power during transit time and improve the UPQC overall performance.

I. INTRODUCTION

The Unified Power Quality Conditioner (UPQC) is a distribution-level controller which is proposed to provide improved power quality in the presence of sensitive loads such as digital electronics, communication systems, and manufacturing processes [1]. UPQC is usually installed at the point of common coupling of industry loads. The UPQC consists of two voltage source inverters (VSI) connected back to back sharing a common DC-link. One inverter acts as a serial dynamic voltage regulator (DVR) whereas the other acts as a shunt active power filter (APF) [2] [3]. The purpose of the serial DVR is to insulate the load against any sags or swells from the source. The purpose of the shunt APF is to filter the harmonic content of the load to keep the source side current clean. Conventionally the DC-link voltage is maintained by the shunt APF exchanging active power with the system. Recently the Energy Storage System (ESS) such as Ultracapacitors is applied into the UPQC DC-link, which can provide high pulse power during transit states. The topology of UPQC with ESS is shown in Figure 1.

Ultracapacitors (UCAP) are electrical energy storage devices which offer high power density and high cycling capability. It can be used as a rapid discharge energy storage for power applications. UCAP has been used extensively in pulsed power applications for high-energy physics and weapons applications. Ideal power system applications for UCAP are short duration storage applications such as power stabilization, power quality ride-through applications, and voltage flicker mitigation among other applications that require high power density and rapid recharge. The major difference between an UCAP compared to a conventional capacitor is that the liquid electrolyte

structure and porous electrodes give the UCAP a high effective area that minimizes the distance between the two plates. Additionally, UCAP has cells that can be connected in serial and parallel to obtain the desired voltage level and capacitance [4]. By utilizing a bidirectional DC/DC converter, the UCAP is an attractive solution for UPQC to provide large amounts of short term active power. The DC/DC converter topology with UCAP is shown in Figure 2.
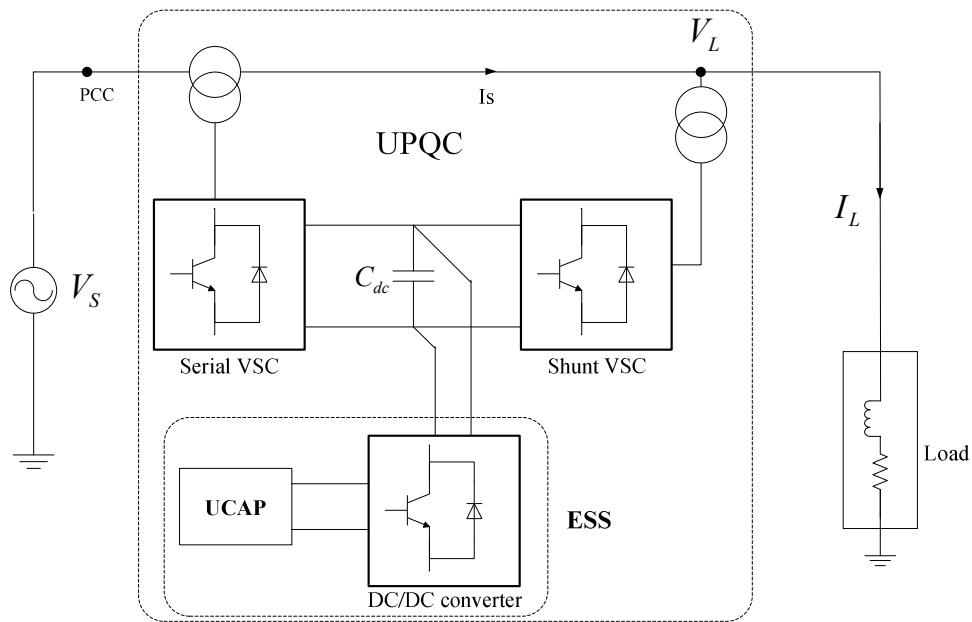

Fig. 1 UPQC with DC/DC converter and UCAP

The DC/DC converter can make the DC bus voltage independent on the voltage of the UCAP. As a result, the DC bus voltage can be controlled to be constant, and the UCAP can be efficiently used with a big voltage variation, around 100% to 50% of the voltage rating. The UCAP based DC/DC converter control scheme is divided into BUCK

and BOOST mode separately. When the UPQC is working in the transient state, the converter operates as a boost converter, which transfers the stored energy from UCAP to DC link and maintains a stable DC link voltage. In the steady state, the converter will take some time to work as a buck converter, which pulls the energy of DC link to recharge the UCAP. Normally at any instant only one IGBT of the converter works. In boost mode, S2 is working and S1 is off. In buck mode, S1 is working and S2 is off. To guarantee the power flowing smoothly both ways and to avoid instantaneous impact upon DC link capacitor and the two IGBTs, a state of idle mode is used to switch between buck and boost mode, which keeps both S1 and S2 off.

With UCAP the UPQC has an optimized power flow between UPQC and system during the transit state, shown in Section II. Also the UPQC's DVR and APF part has an improved performance with UCAP, shown in Section III. Furthermore, the UCAP character is experimentally analyzed and its equivalent circuit model is built up in Section IV. The impact of UCAP model on its control and simulation is analyzed in Section V. From the analysis, UCAP based Energy Storage System can well fulfill the requirement of UPQC to provide high active power during transit time, and improve the UPQC overall performance.

With UCAP the UPQC has an optimized power flow between UPQC and system during the transit state, shown in Section II. Also the UPQC's DVR and APF part has an improved performance with UCAP, shown in Section III. Furthermore, the UCAP character is experimentally analyzed and its equivalent circuit model is built up in Section IV. The impact of UCAP model on its control and simulation is analyzed in Section V. The UPQC compensation limit with the selected UCAP size is shown in

Section VI. From the analysis, UCAP based Energy Storage System can well fulfill the requirement of UPQC to provide high active power during transit time, and improve the UPQC overall performance.
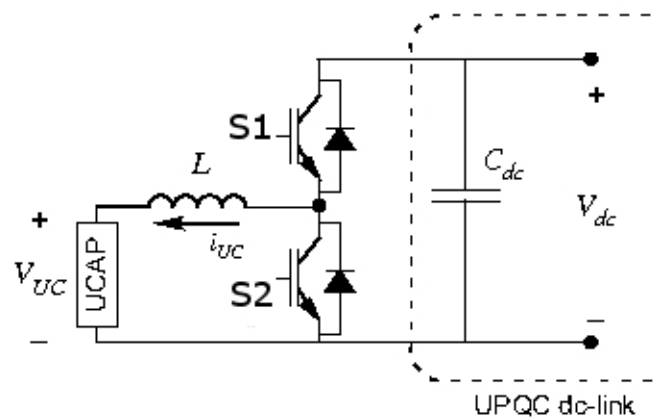

Fig. 2 DC/DC converter with UCAP

II. OPTIMIZED UPQC POWER FLOW WITH UCAP

The UPQC needs to inject active power into the system to maintain the load bus voltage level during voltage sag. Conventionally the active power exchange is realized by shunt APF to maintain the DC-link voltage. To show the advantage of the new UPQC topology with UCAP, Figures 3 - 5 make an analysis of UPQC power flow with and without UCAP. The vectors shown in the figures are in $\begin{bmatrix} P \\ U \\ I \end{bmatrix}$ format, representing active power flow, voltage and fundamental frequency current in per unit value. The load side is desired to maintain in $\begin{bmatrix} 1 \\ 1 \\ 1 \end{bmatrix}$ profile. In each figure, the vectors are given at point A for source side, point B for the internal UPQC and point C for the load side. The vector at point D is for DVR output, and the vector at point E is for APF output.

In the conventional UPQC without UCAP, if the source side voltage Vs drops to "x", the power flow is as Figure 3. If Vs drops to 0.5 p.u. (x=0.5), the current at DVR output is 2 p.u. $(\frac{1}{x})$ and the current at APF output is 1 p.u. $(\frac{1}{x} - 1)$. The current in the primary side of the serial transformer is 2 p.u. $(\frac{1}{x})$. This means the power flow in UPQC is dramatically increased during the source voltage sag.

If the UPQC is equipped with UCAP, when Vs drops to "x", the power flow is as Figure 4. Since the current in APF has no fundamental frequency part, so APF has no active power flow shown as in dash line. If Vs drops to 0.5 p.u., the current at DVR

output is 1 p.u. and the fundamental frequency current at APF is zero. The current in the

primary side of the serial transformer is 1 p.u.. The power flow is much smaller than the

UPQC without UCAP topology as in Figure 3 during the transit state.
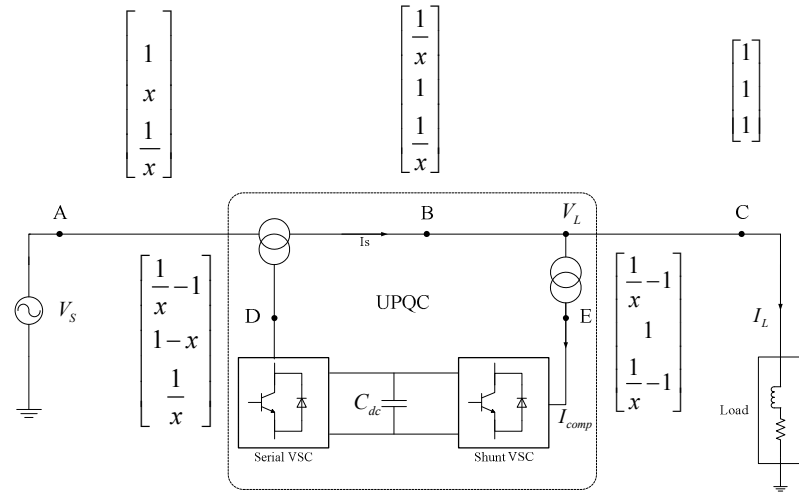
Fig. 3 UPQC power flow without UCAP during voltage compensation
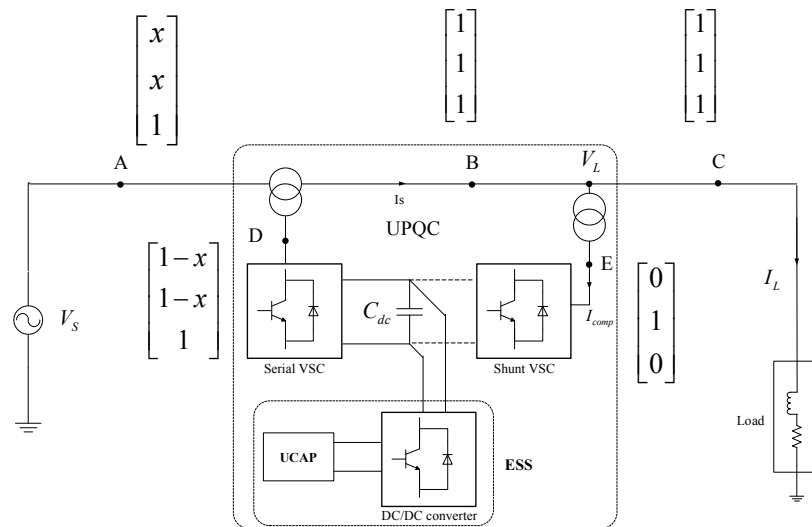
Fig. 4 UPQC power flow with UCAP during voltage compensation

32

In the UPQC with UCAP topology, during the UCAP recharging mode the power flow is as Figure 5. "y" is the charging current magnitude which can be chosen freely. If the charging current y is 0.1 p.u., the current at DVR output is only 1.1 p.u. and the current at APF output is 0.1 p.u.. The current in the primary side of the serial transformer is 1.1 p.u.. By choosing smaller charging current the active power flow can be very small during the recharging mode.
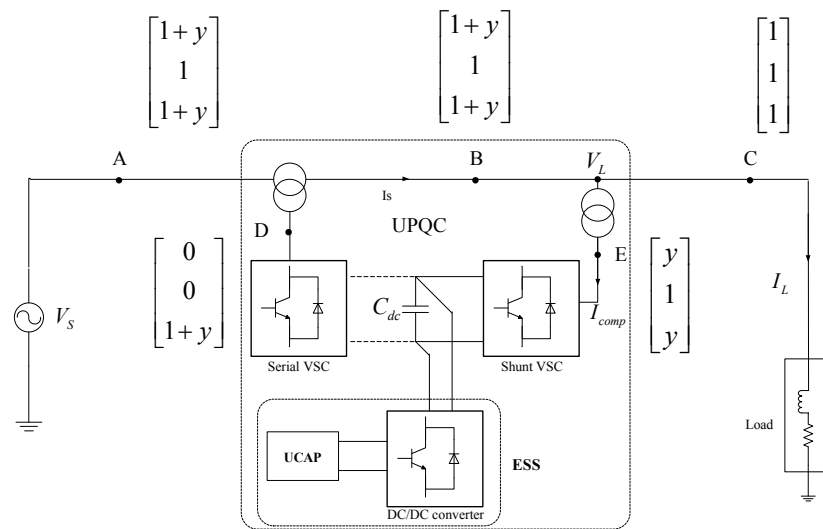
Fig. 5 UPQC power flow with UCAP during recharging mode

The simulation results also verify the optimized power flow. Figure 6 shows the power flow comparison without and with UCAP when Vs drops to 0.5 p.u.. The UPQC is applied to a 5MW load. During the fault without UCAP the power flow in UPQC is two times of the UPQC with UCAP. Figure 7 also shows the power flow during the UCAP

recharging mode. The UCAP is recharged from 1.45kV to 1.5KV from 0.4s to 0.7s. The result shows there is small power flow during the recharging mode.

Fig. 6 UPQC power flow simulation comparison without and with UCAP

Fig.7 UPQC recharging mode simulation with UCAP

Figures 3 - 7 show that with UCAP, lower active power and current flow through UPQC device during voltage sag. It means the switch devices such as IGBT in UPQC can choose smaller power rating, and the cost of UPQC is reduced.

III. UPQC PERFORMANCE IMPROVEMENT WITH UCAP

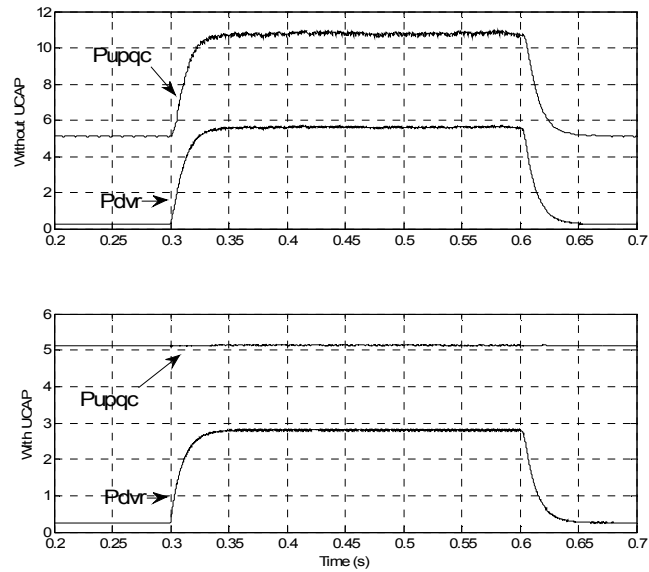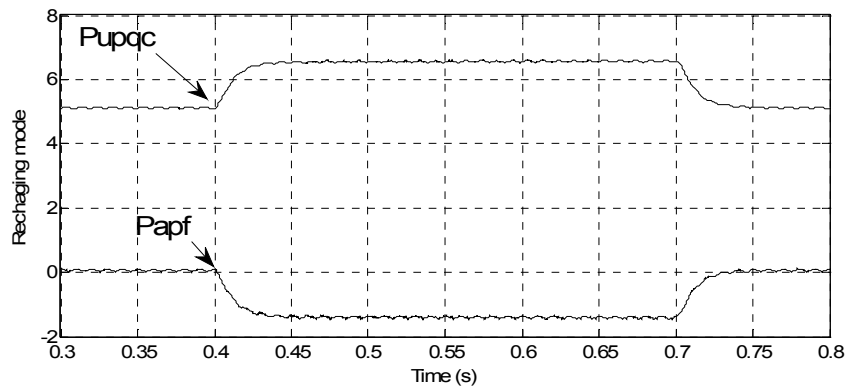Since the two UPQC inverters have significantly different objectives, UPQC control is accomplished by considering the serial DVR and shunt APF inverter control separately. The detail benefits of UCAP for UPQC are shown in these two parts. The UPQC simulation environment is built in EMTDC/PSCAD.

A. UPQC DVR Part

The UPQC DVR part is devoted to dynamic voltage regulation. It enables the voltage seen by the load to be unchanged during voltage excursions upstream. Two typical control schemes for the DVR are the in-phase and the phase-shift control methods.

These two approaches are illustrated in Figure 8. To achieve the same magnitude output voltage V_L, a voltage can be injected in-phase with the source voltage (V_{inj1}) or at an angle shifted from the source voltage (V_{inj2}). While the in-phase injected voltage magnitude is smaller than the phase-shift injected voltage, the required active power injection is greater. This is the primary difference between the two basic control approaches. In addition, the phase-shift compensation causes the load voltage phase angle to shift during compensation. Since sensitive loads such as induction motors and adjustable speed drives are very sensitive to deviations in phase angle shift, this introduces large transient currents into the stator circuit of the motor, which results in greater losses, temperature rise, and possibly damage to the IGBTs [5]. The dynamic response to a three-phase ground fault of the UPQC DVR part under both control

approaches is shown in Figures 9 and 10. In these figures, Is is the source current, Vs is the source voltage, Vinj is the DVR output voltage, Pinj is the DVR output active power, Vdc is the DC-link voltage. The fault lasts 0.1 seconds during which the system bus voltage sags to 0.5 p.u..

With the in-phase control, the load voltage can not be fully compensated because there has no enough active power from DC-link. It drops significantly. The phase-shift control, while having better load voltage control, shows significant high-frequency transients in the load current and bigger injection voltage magnitude. The advantages and disadvantages of the two control methods are summarized in Table 1.

From the comparison, the only disadvantage of the in-phase control method is the larger amount of injected active energy required. In the conventional UPQC topology APF is only able to compensate for a limited amount of active power [6], therefore another energy source needs to be added into UPQC DC-link as Energy Storage System (ESS). Integrating an UCAP through a bi-directional DC/DC converter is applied to fulfill the requirement.

With the UCAP based ESS, the results of the in-phase compensation with the UCAP is shown in Figure 11. The in-phase control method overcomes the stated limitations since additional energy can be pulled from the UCAP during voltage sag. The high-frequency transients in the current and voltage magnitude have been eliminated. In addition, the magnitude of the injected voltage is decreased over the non-UCAP phase-shift control method. In addition, the phase-shift compensation with the UCAP is shown in Figure 12. The results show that with enough energy storage system, if still using phase-shift method the UPQC can work normally but the shortcomings of phase-shift

method are also shown in the result, such as transient current. So the phase-shift method is not necessary for UPQC with UCAP.
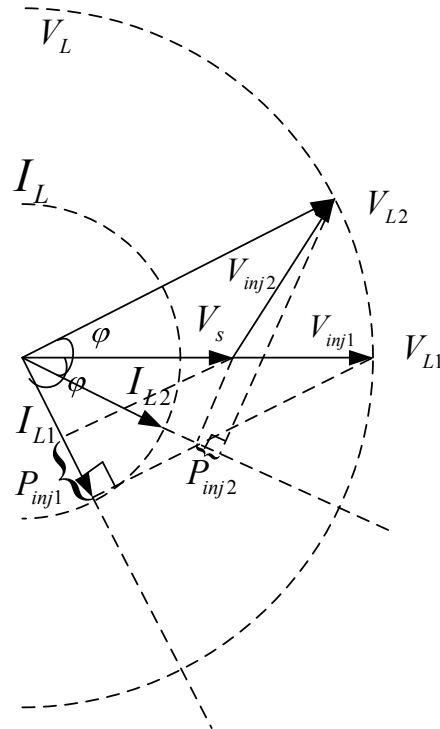

Fig. 8 UPQC DVR part control region

With the UCAP based ESS, the results of the in-phase compensation with the UCAP is shown in Figure 11. The in-phase control method overcomes the stated limitations since additional energy can be pulled from the UCAP during voltage sag. The high-frequency transients in the current and voltage magnitude have been eliminated. In

addition, the magnitude of the injected voltage is decreased over the non-UCAP phase-shift control method. In addition, the phase-shift compensation with the UCAP is shown in Figure 12. The results show that with enough energy storage system, if still using phase-shift method the UPQC can work normally but the shortcomings of phase-shift method are also shown in the result, such as transient current. So the phase-shift method is not necessary for UPQC with UCAP.

Table 1.Comparison between in-phase and phase-shift control methods

	In-phase	Phase-shift
Advantage	Lower injected voltage	Lower injected energy
Disadvantage	Higher injected energy	Higher injected voltage Current transients

B. UPQC APF Part

The shunt inverter in UPQC acts as an active power filter (APF) to mitigate the impact of the load harmonics on the power system. The source side current is significantly degraded by the impact of the harmonic currents on the load side. The APF injects a compensation current such that off-fundamental frequency harmonics are cancelled and the source current becomes a clean sinusoidal waveform.

Figure 13 and 14 show a comparison of the source, load, and compensating current without and with a UCAP. Without a UPQC, the harmonic content of the load voltage is nearly 20%. The UPQC topology without a UCAP can provide improvement in

the source voltage and the total harmonic distortion drops to 6%, but there are still obvious non-sinusoidal components. With the UCAP, the source voltage is nearly sinusoidal and most harmonic content has been compensated. The total harmonic distortion is around 1%. This improvement comes from the ability of the DC/DC converter to maintain the DC-link voltage, thereby the APF part only needs to eliminate the harmonics without controlling the DC-link voltage.
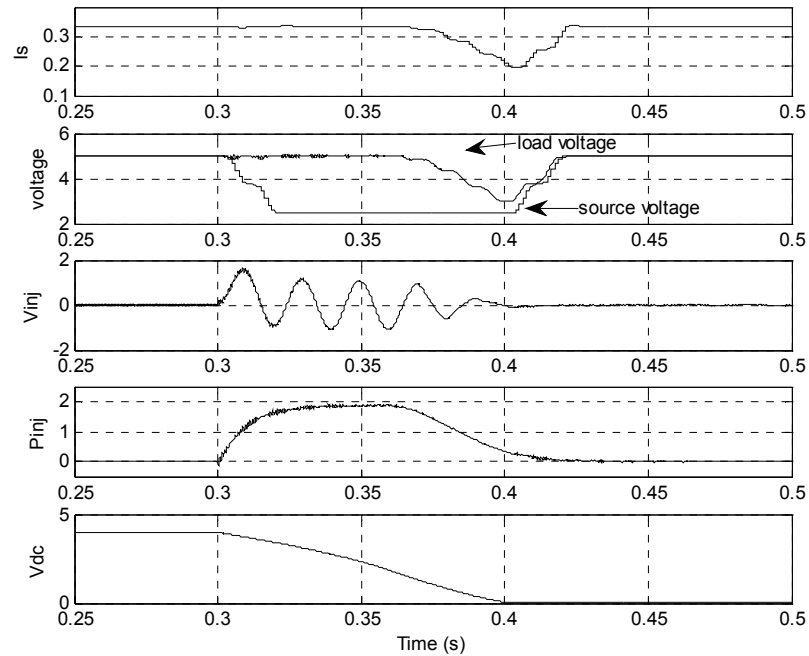

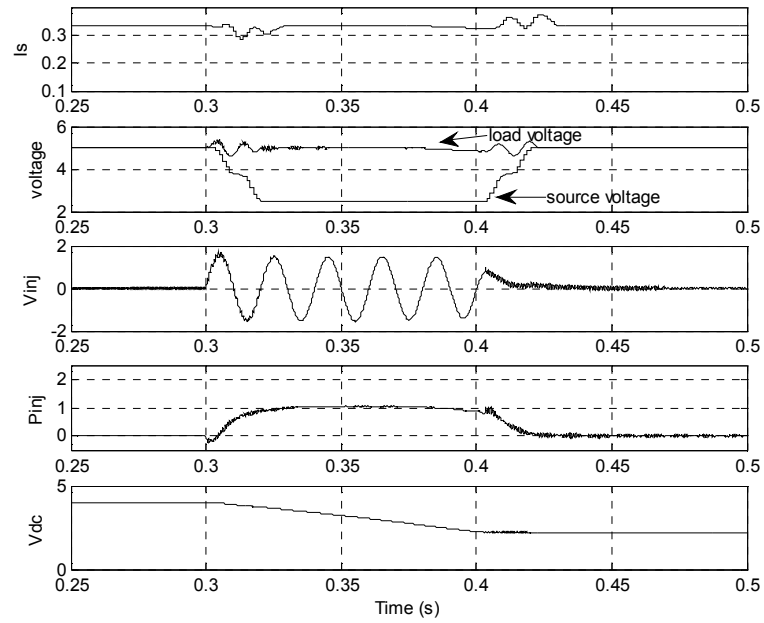Fig. 9 UPQC DVR without UCAP and with in-phase control

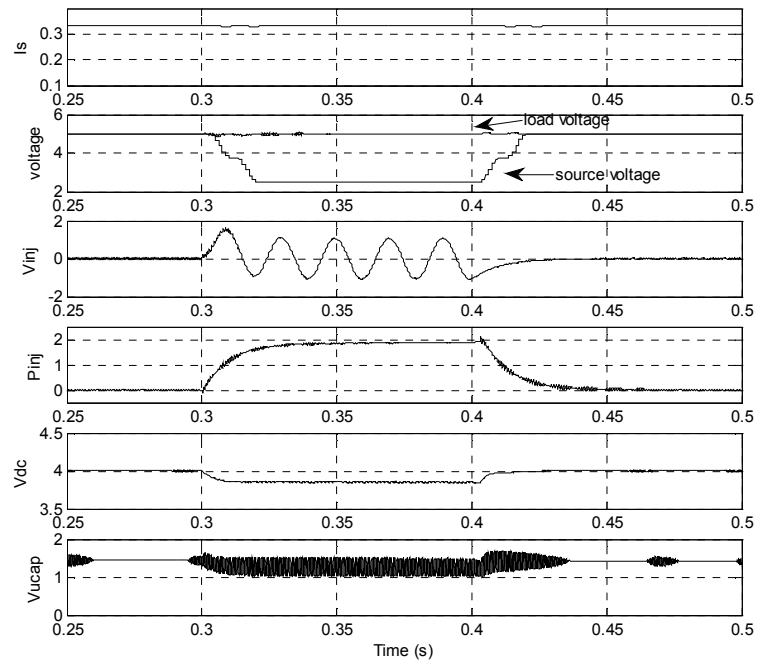Fig. 10 UPQC DVR without UCAP and with phase-shift control

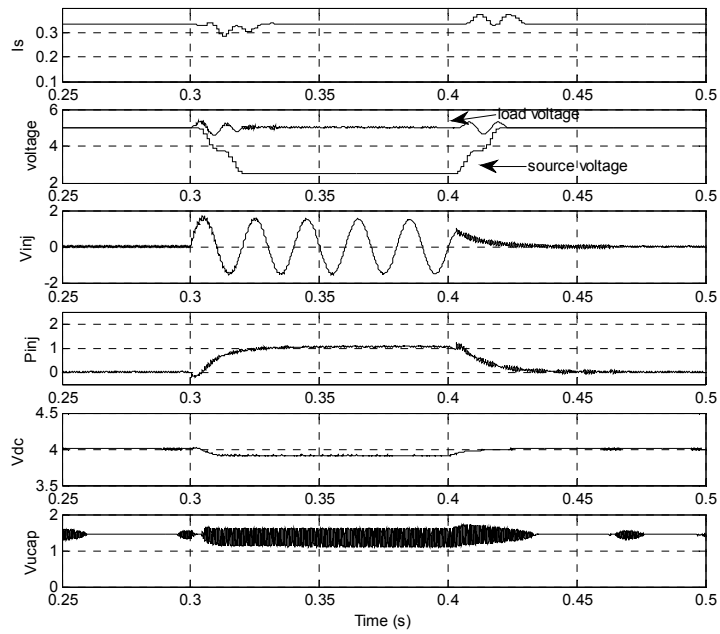Fig. 11 UPQC DVR with UCAP and in-phase control
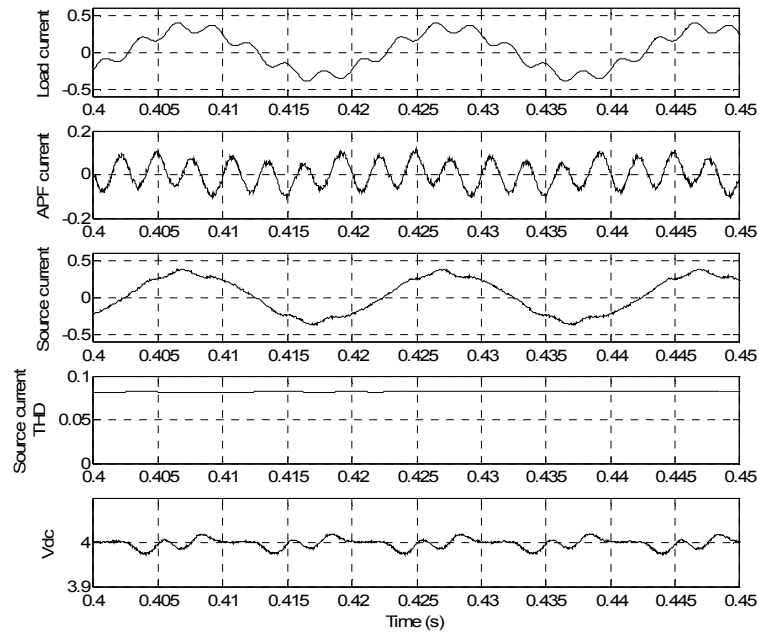
Fig. 12 UPQC DVR with UCAP and in-phase control
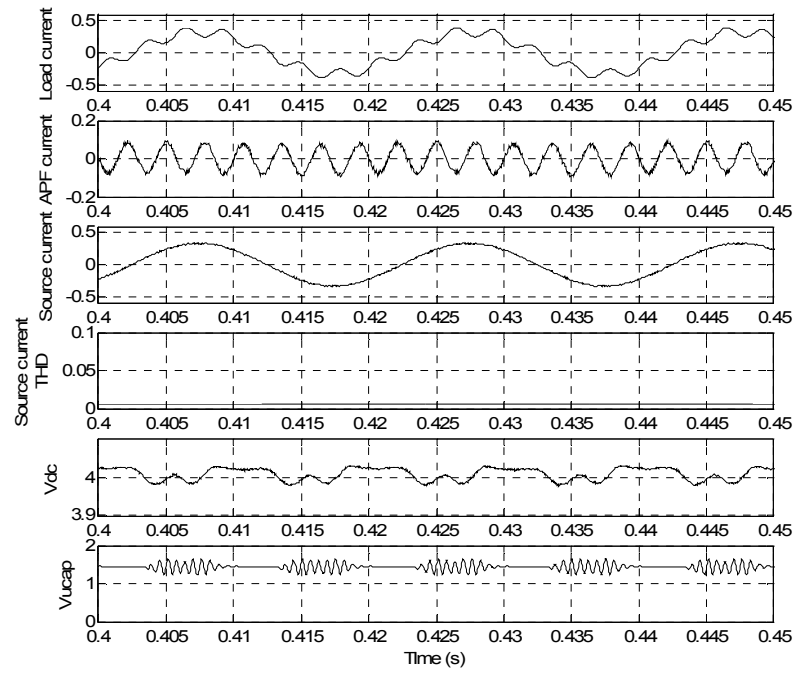

Fig. 13 UPQC APF harmonic elimination without UCAP

Fig. 14 UPQC APF harmonic elimination with UCAP

IV. THE ULTRACAPACITOR

The UCAP is a relatively new device in the energy storage area which offers high power density and extremely high cycling capability [7]. Usually the UCAP manufacture data sheets only list major parameters such as capacitance and series resistance with several constant-current discharge curves [7]-[9], but include little or no transient response information. To optimize the UCAP performance with UPQC, detailed performance information is needed for the UCAP.

Normally UCAP can be presented by various equivalent circuits based on physical phenomena [9]. The most common representation of an ultracapacitor is a single capacitance in series with a resistor as shown in Figure 15. Recent results however, indicate that a distributed or "ladder" circuit provides better indication of the transient behavior of the UCAP [4] [10] [11]. To derive the ladder circuit of the UCAP, frequency analysis is used to measure the complex impedance of the UCAP module. The testing hardware setup of the frequency analysis is shown in Figure 15. The resistors R1 and R2 are adjusted to provide the desired current level through the UCAP (in our case R1=1Ω and R2=100Ω). A signal generator supplies the required driving signal to the IGBT through a standard gate drive circuit. By testing the current and voltage response of the UCAP over a wide range of frequencies, the magnitude and phase of UCAP impedance can be extracted.
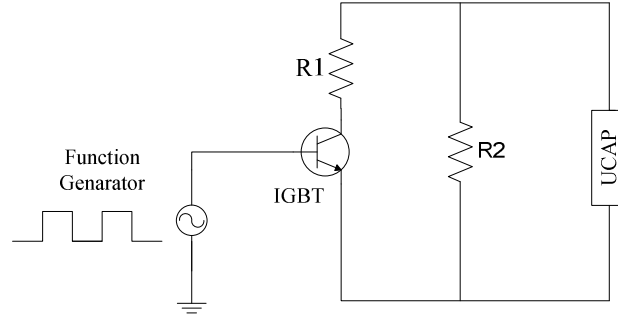
Fig. 15 UCAP frequency analysis circuit

The test current and resulting voltage at 60 Hz are shown in Figure 16. Note that even though the current variation is quite large, the UCAP voltage variation is still relatively small due to the large capacitance of the UCAP. The resulting UCAP Bode plot is shown in Figure 17. The frequency is varied from 0.001 Hz to 10,000 Hz. This figure shows that there are mainly three separated character bands for UCAP. The capacitance of the UCAP dominates in the low frequency band. The equivalent series resistance (ESR) of the UCAP dominates in the mid frequency band and the inductance begins to dominate in the high frequency.

Based on the measured experiment data, an alternate frequency relationship can be obtained from the Nyquist plot which displays the real versus imaginary impedance components as a function of frequency. The Nyquist plot of the UCAP module in the 0.1 Hz to 500 Hz range is shown in Figure 18. The frequency response of the UCAP ladder circuit transfer function [12].

$$Z(s) = \frac{b_n s^n + b_{n-1} s^{n-1} + \ldots + b_1 s + b_0}{s^n + a_{n-1} s^{n-1} + \ldots + a_1 s + a_0} \tag{1}$$

(Where n is the number of RC sub-circuits in the ladder) can be used to determine the order and parameters of the ladder circuit by curve fitting. By using a nonlinear least-squared-error minimization, the fitting curves shown in Figure 18 were obtained for first through fourth order ladder circuits. The first order circuit results in a poor fit. This implies that the traditional first order equivalent circuit model of a single resistance and capacitor may produce erroneous dynamic results over a wide range of frequencies. The results of the second through fourth order models provide a much better fit. The residual norms of the nonlinear curve fitting are given in Table 2. Since the residual norm does not change much between the third and fourth order models, the ladder circuit can be truncated with this number of sub-circuits.

The UCAP is connected to UPQC with a DC/DC converter. For the best efficiency of DC/DC converter, UCAP voltage level is 1.5kV when the UPQC DC-link voltage is 4kV [13]. The UCAP module's rating is 330F with 30V. Since the performance of a capacitor is an inherent property and it depends only on the construction materials and the cell design. Series or parallel connecting these capacitors does not change the resulting performance [14]. In the simulation 50 modules are parallel connected together and the UCAP module parameters multiply 50 times to get the demand level. After combination, the resulting fourth-order ladder circuit is shown in Figure 19.
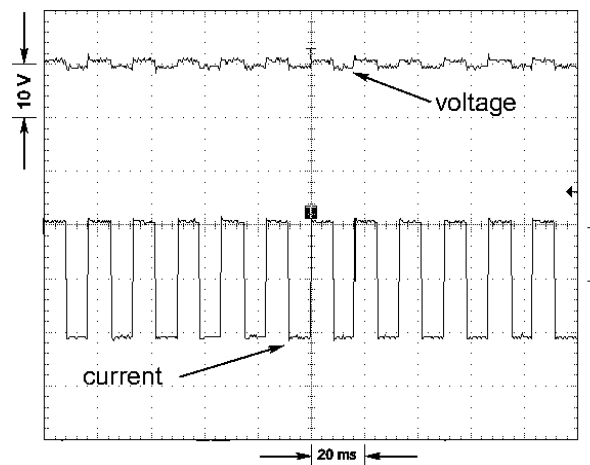
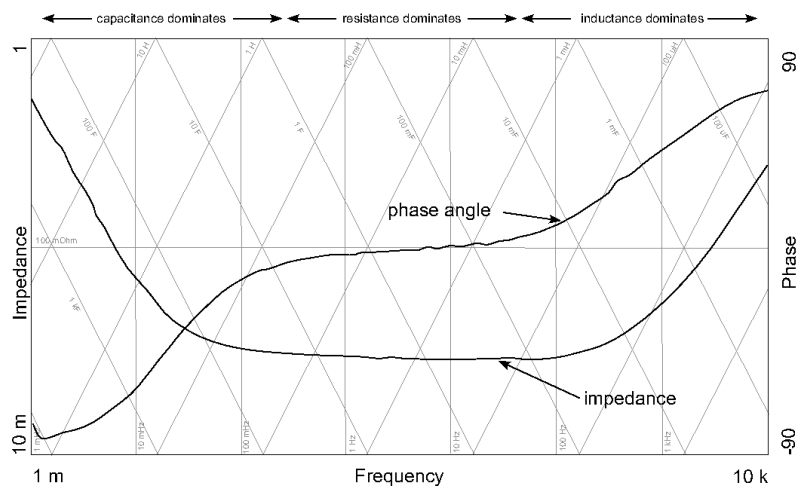Fig. 16 Testing current and voltage for the UCAP

Fig. 17 Bode plot of UCAP model frequency analysis
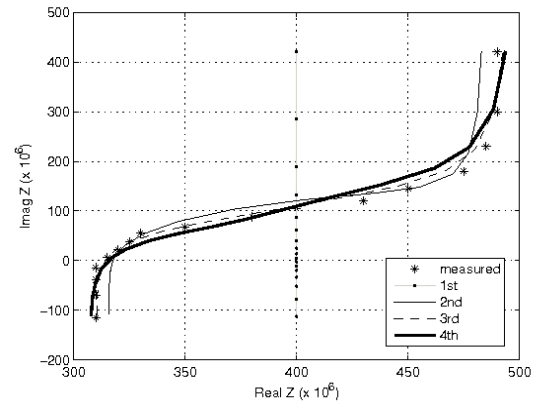
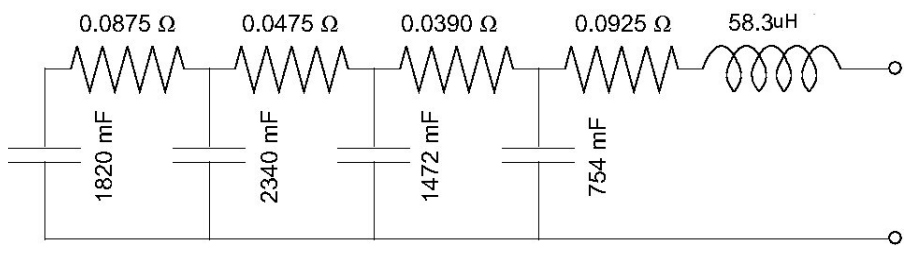Fig. 18 Fitted ladder circuit frequency response (0.1Hz-500Hz)

Fig. 19 Fourth order model of UCAP

Table 3. Ladder circuit residual norms

Order	Error ($*10^{-6}$)
Second	44.52
Third	29.06
Fourth	27.76

V. IMPACT OF UCAP MODEL ON COTROL AND SIMULATION

Different models of UCAP can lead to varying degrees of accuracy in simulation and control development. In this section, a brief comparison of the effects of the standard first-order and the fourth-order model of the UCAP on the UPQC performance is provided.

A. Series Inductance

Manufacturer data sheets typically only provide the ESR and the power frequency capacitance of the UCAP for the first-order model. However, the series inductance has a significant impact on the behavior of the UCAP during transients. The UCAP terminal voltage has considerable variation due to the large $L\dfrac{dI}{dt}$ which makes it unsuitable for control signal input. To be used as a control signal input for the DC/DC converter, a low pass filter for UCAP terminal voltage measurement is required. Figure 20 shows the difference between a model with and without the series inductance and the terminal voltage after filtering.

B. Equivalent Series Resistance

The fourth order model yields a ladder circuit with different internal resistance compared to the traditional first-order model. This difference in resistances leads to a small, but significant difference in time constant response of the UCAP and power consumption. In the steady-state, the UCAP provides voltage support through the DC/DC converter to compensate the UPQC steady state losses and make the DC-link voltage

stable (as shown in Figure 10). This requires a continual small active power drain on the UCAP; therefore the UCAP is periodically recharged. The comparison of the first and fourth order boost-buck-boost mode operation is shown in Figure 21. When the UCAP voltage drops to 1.4 kV, the DC/DC converter switches to buck mode to bring the UCAP voltage back to the reference voltage of 1.5 kV. In the first order model, UCAP voltage drops from 1.5kV to 1.4kV and it takes 30s. In the fourth order model, UCAP voltage drops from 1.5kV to 1.4kV and it takes 31.4s. The fourth order model UCAP indicates that the cycle time between recharges is slightly longer than for the first order traditional model. For the same working voltage range, the fourth order model can support the steady state longer.
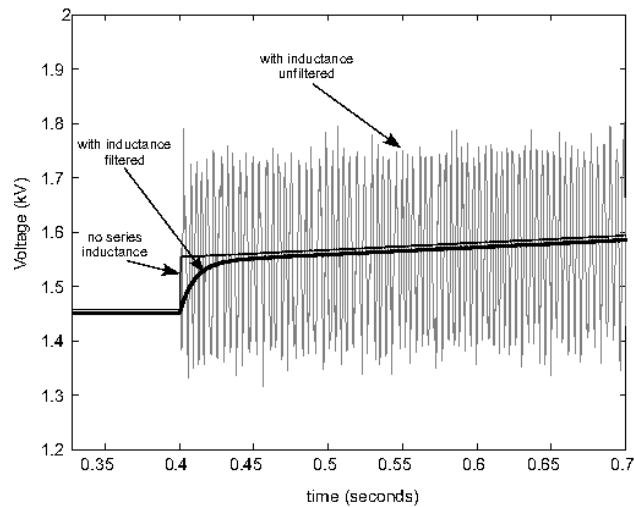
Fig. 20 UCAP model voltage with and without series inductance
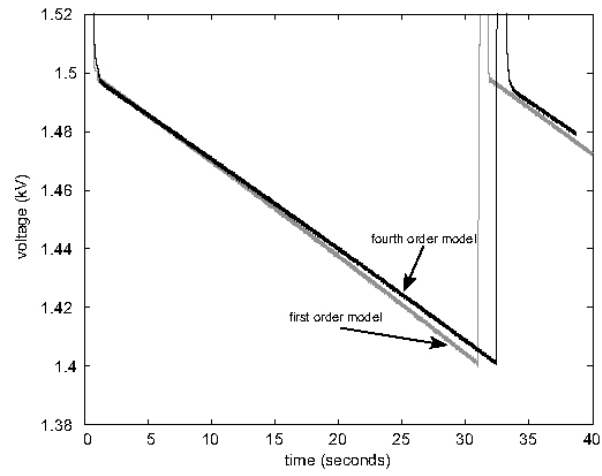
Fig. 21 Boost-buck-boost switching cycle

VI. UPQC COMPENSATION LIMIT WITH SELECTED UCAP

The UPQC is a distribution-level power quality device. This section shows the UPQC has a compensation limit with the selected UCAP size. For a typical distribution power system, the bus voltage rating is 5kv and load rating is 5MW. The UPQC DC-link voltage level is selected as 4kV and the UCAP voltage level is 1.5kV. The system parameters are summarized in Table 3.

Table 3. Test system parameters

System bus voltage (Vs)	8.66 kV (L-L)
DC-link voltage (Vdc)	4 kV
DC-link capacitor (Cdc)	4 mF
UCAP voltage (Vucap)	1.5 kV
UCAP capacitor (Cucap)	6 F

A. DVR Part Compensation Limit

The DVR voltage output in PWM control scheme is:

$$V_o = T \cdot ma \cdot V_{dc} \tag{2}$$

ma is demand modulation signal, 0<ma<1. T is series transformer ratio, here is 5:10.

If UPQC has an ideal DC energy storage, it has enough energy delivery during the fault time. DVR compensation limit is only depends on Vdc. If Vdc=4kV, DVR output Vo has enough compensation range for any sag for a 5kV bus voltage system.

The boost converter connecting UPQC DC-link and UCAP has a voltage output with duty ratio D.

$$V_{dc} = \frac{1}{1-D} \cdot V_{ucap}$$ (3)

Due to the effect of parasitic resistances in the boost converter, it has a maximum voltage and power output at certain duty ratio D [13]. In case of system fault, the equivalent load resistor is small and the boost converter has a limited voltage and power output. The simulations are performed under different voltage sag conditions.

When Vs drops to 0.4 p.u., the simulation result is shown in Figure 22. The load voltage can be restored with UCAP support. When Vs drops to 0.3 p.u., The simulation result is shown in Figure 23. The load voltage can not be fully restored with UCAP support. In summary with selected UCAP size the DVR can compensate 60% voltage sag. The compensation limit comes from the maximum power output of boost converter.

In the voltage swell condition, DVR injects voltage in reverse direction to eliminate the voltage swell. DVR absorbs energy from system and makes the DC-link voltage rise up. The DC voltage control scheme in APF is applied to maintain the DC-link voltage level. In this condition DVR can compensate any voltage swells. Figure 24 shows the simulation result when source voltage swells to 1.5 p.u..
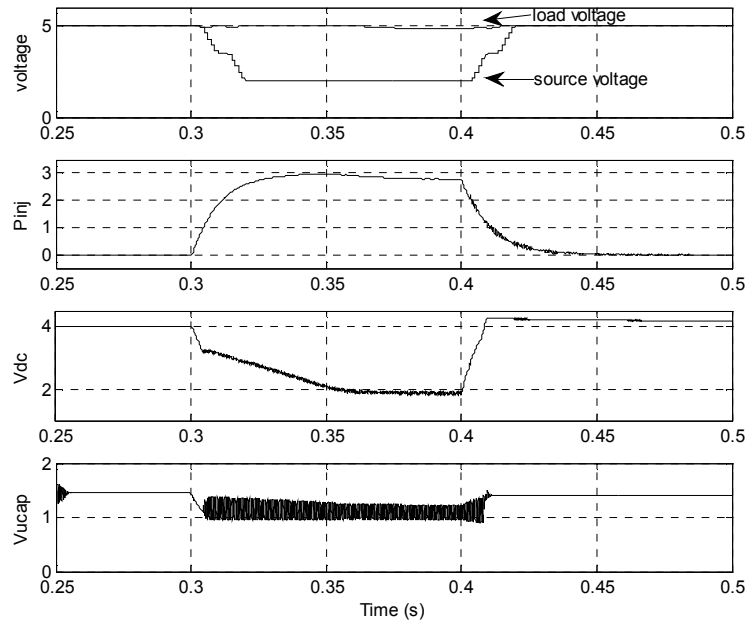
Fig. 22 DVR compensation when Vs drops to 0.4 p.u.
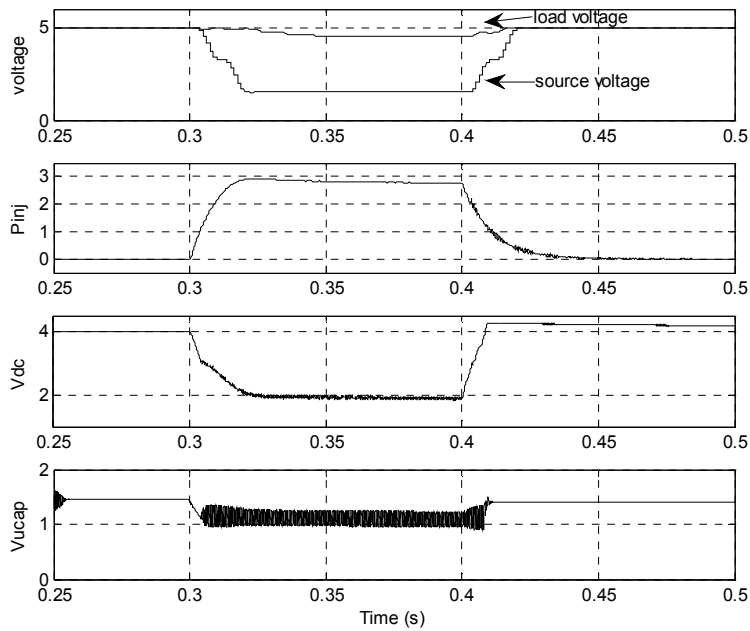
Fig. 23 DVR compensation when Vs drops to 0.3 p.u.
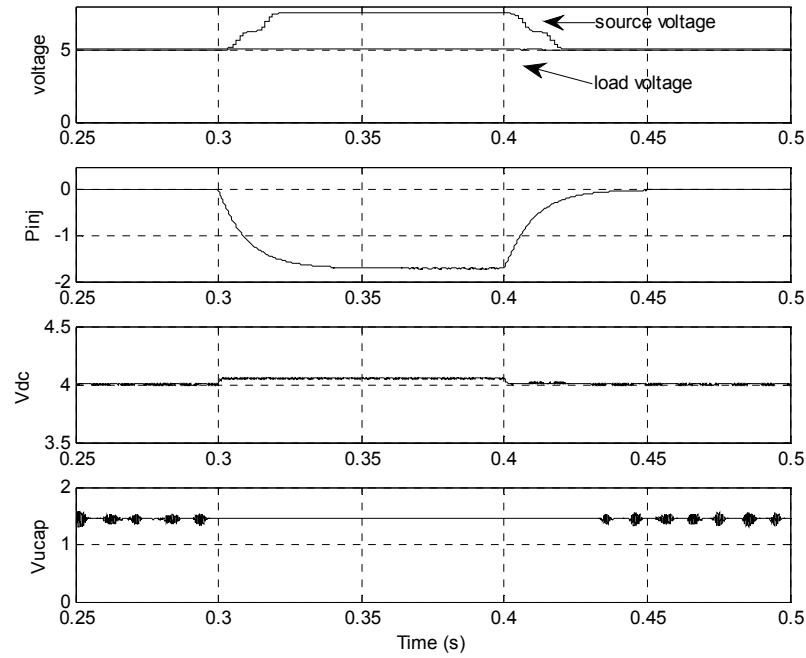
Fig. 24 DVR compensation when Vs swells to 1.5 p.u.

B. APF Part Compensation Result

Since APF consumes very little active power, its compensation result only depends on DC-link voltage magnitude Vdc. The design principle of choosing a suitable Vdc for APF is based on the trade-off between an undistorted input current waveform and a minimum switching loss [15]. For better harmonic elimination result, Vdc should be set higher. However, the switching loss of the APF will increase at the same time, and higher Vdc makes higher cost of UCAP. The demanding Vdc level is calculated by:

$$V_{dc} \geq T \cdot (V_s + L_{apf} \cdot M_{max}) \tag{4}$$

Vs is source voltage magnitude; Lapf is APF connecting inductor; Mmax is the maximum slope of current harmonics. T is the connecting transformer ratio.

Fig. 25 APF performance when Vdc is 2.5kV
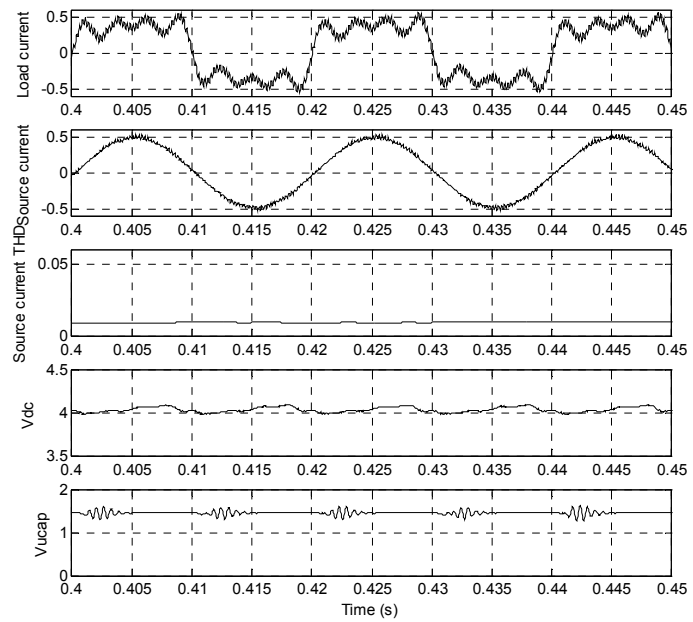
Fig. 26 APF performance when Vdc is 4kV

The simulations of APF performance with different DC-link voltage are shown in Figure 25 and Figure 26. When Vdc is 2.5kV source current THD is dropped to 3%. When Vdc is 4kV source current THD is dropped to 1%. Higher Dc-link voltage has better current harmonic elimination result.
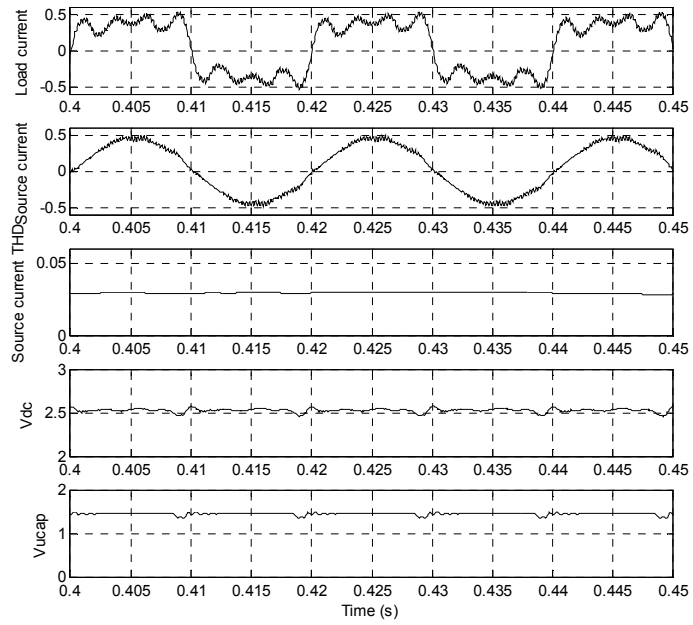
VII. CONCLUSIONS

This paper presents an analysis of the UPQC connected with UCAP through a DC/DC converter. In the new topology the optimal power flow is realized. The UPQC/UCAP is shown to offer improved performance over a normal UPQC without additional energy storage system. The UPQC/UCAP is better able to maintain the load voltage during transients; the total harmonic distortion is decreased. The impact of the different UCAP models on its performance is discussed in relation to the appropriate order of the ladder circuit. The traditional first order model given by the manufacturer is insufficient to adequately represent the possible behavior and losses of the UCAP during UPQC operation. Higher order UCAP model is more accurate for simulation and control development. The UPQC compensation limit with selected UCAP size is also analyzed.

VIII. ACKNOWLEDGMENTS

IX. REFERENCES

1. Dorr, D., Hughes, M., Gruzs,T., Jurewicz, R., and McClaine, J., "Interpreting recent power quality surveys to define the electrical environment," IEEE Trans. on Industry Applications, vol. 33, no. 6, November/December 1997, pp. 1480-1487.

2. Fujita, H., and Akagi, H., "The Unified power quality conditioner: The Integration of series- and shunt-active filters," IEEE Trans. on Power Electronics, vol. 13, no. 2, March 1998, pp.315-322.

3. Khadkikar, V., and Chandra, A., "A new control philosophy for a unified power quality conditioner (UPQC) to coordinate load-reactive power demand between shunt and series inverters," IEEE Trans. on Power Delivery, vol. 23, no. 4, October 2008, pp.2522-2534.

4. Atcitty, S., Electrochemical Capacitor Characterization for Electric Utility Applications, Ph.D. Dissertation, Virginia Tech, 2006.

5. Li, J. D., Choi, S. S., and Vilathgamuwa, D., "Impact of load transients on dynamic voltage restorers," Proceedings of the 2002 International Conference on Power System Technology (PowerCon), Kunming, China, vol. 1, 2002, pp.464-470.

6. Ng, F., Wong, M., and Han, Y., "Analysis and Control of UPQC and its DC-Link Power by Use of p-q-r Instantaneous Power Theory," IEEE 1st. International Conference on Power Electronics Systems and Applications, November 2004, pp.43-53.

7. Bullard, G. L., Sierra-Alcazar, H. B., Lee, H. L., and Morris, J. L., "Operating principles of the ultracapacitor," IEEE Trans. on Magnetics, vol. 25, January 1989, pp. 102-106.

8. Schempp, E., and Jackson, W. D., "Systems considerations in capacitive energy storage," Proceedings 31st Intersociety Energy Conversion Engineering Conference, vol. 2, August 1996, pp. 666-671.

9. Bonert, R., and Zubieta, L., "Measurement techniques for the evalution of double-layer power capacitors," Proceedings of the 1997 Industry Applications 32nd Annual Meeting, October 1997, pp. 1097-1100.

10. Nelms, R. M., Cahela, D. R., and Tatarchuk, B. J., "Modeling double layer capacitor behavior using ladder circuits," IEEE Trans. on Aerospace and Electronic Systems, vol. 39, no. 2, April 2003, pp.43-438.

11. Buller, S., Karden, E., Kok, D., and De Doncker, R. W., "Modeling the dynamic behavior of supercapacitors using impedances spectroscopy," IEEE Trans. on Industry Applications, vol. 38, no. 6, November/December 2002, pp. 1622-1626.

12. Shi, L., and Crow, M. L., "Comparison of Ultracapacitor Electric Circuit Models," Proceedings of the 2008 IEEE Power & Energy Society General Meeting, July 2008, pp. 1-6.

13. Erickson, Robert W., and Maksimovic, Dragan, "Fundamentals of Power Electronics," Kluwer Academic Publishers, 2001

14. Miller, John R., "Development of Equivalent Circuit Models for batteries and Electrochemical Capacitors," The Fourteenth Annual Battery Conference on Applications and Advances, 1999, pp. 107-109.

15. Lo, Yu-kang, Pan, Tian-Fu, and Wang Jian-Min, "Setting the DC voltage level of an active power filter," International Journal of Circuit Theory and Applications, 2008, pp. 975-982.

PAPER III

UPQC with Energy Storage System Performance Comparison by using PI and H∞ Method

Xiaomeng Li, Mariesa L. Crow
Electrical and Computer Engineering
Missouri University of Science and Technology
Rolla, MO 65409

ABSTRACT

Unified Power Quality Conditioner (UPQC) with Energy Storage System (ESS) is widely used in power distribution system. Conventionally the PI control method is applied in UPQC control scheme, including DVR and APF part. Recently the H∞ control method is widely applied in Power Quality area. This paper shows the two control schemes and their performance comparison under different load conditions. The simulation results show that the two methods have their own advantages and disadvantages. In the practical application the control method can be chosen by considering the different application area.

Keywords

UPQC, Power Quality, Instantaneous reactive power theory, H∞ control method.

I. INTRODUCTION

With the increase of the complexion in the power distribution system, it is very possible that several kinds of power quality disturbances are happened in a power distribution system simultaneously. Loads such as diode converters produce large harmonics interferences. Voltage disturbance is also a big problem for sensitive consumers. In order to improve the reliability and efficiency of power distribution system, it is important to introduce UPQC (Unified Power Quality Conditioner) as a distribution-level controller for Custom Power Quality [1] [2] [3]. UPQC is mostly configured by using the two voltage source converters (VSC), which are connected to power grid in shunt and series. The two converters share with a common DC-link. Multiple power quality regulation functions are implemented in UPQC simultaneously with a high performance ratio. Figure 1 show a typical main circuit topological structure of UPQC, the inner part of imagined line is UPQC, which is composed by series unit and shunt unit as well as DC storage unit. The series unit has the functions of DVR (Dynamic Voltage Restorer), while the shunt unit has the functions of APF (Active Power Filter), and the energy storage unit such as super capacitor has the functions of ESS (Energy Storage System), which can provide very high power during transit states.

Conventionally the PI control method is applied in UPQC control scheme, including DVR and APF part. Recently the H∞ control method is widely applied in Power Quality area [4]. This paper shows the control schemes of PI and H∞ method in UPQC, and their performance is compared under different conditions. In the practical

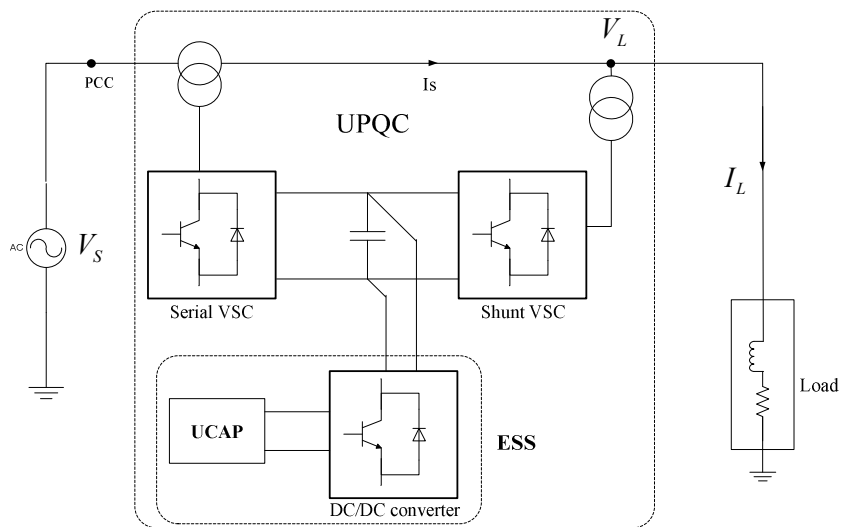application the control method can be chosen by considering the different application area.

Fig. 1 Typical main circuit of UPQC with ESS

II. PI CONTROL METHOD FOR UPQC

A. DVR Part Control

The control of DVR is in a straight forward way. Three phase source voltages (Ua, Ub, Uc) at the UPQC input are feedbacked for fault detection [5]. With the Phase Locked Loop (PLL), a three-phase reference signal is generated for comparison. During voltage sag, this reference system is compared with source voltages in order to produce the control signals (Ua1, Ub1, Uc1). These control signals are adjusted in magnitude by the DC-link voltage and a scaling factor K. After adjustments the control signal passes through the modulator where the PWM signals are generated. These signals are transmitted to the IGBT gates. Figure 2 is the DVR control scheme.
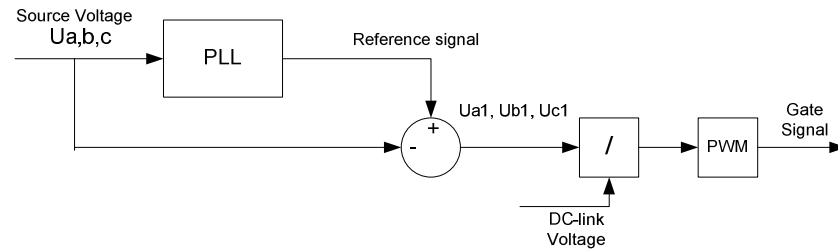
Fig. 2 DVR PI control scheme

B. APF Part Control

In the conventional APF part control, the three-phase harmonic detection method is based on the instantaneous reactive power theory [6]. The three-phase signals are

transferred to two-phase signals in αβ orthogonal coordinates, then to do the further

calculation. A modified single-phase control scheme based on instantaneous reactive

power theory is used here in UPQC and extended to the three phase topology [7].

In single-phase circuit, a lagging current signal is constructed which is lagged to

the practical current T/4 (T is the fundamental cycle), to directly form the supposed

signals in two-phase αβ coordinates. According to the instantaneous reactive power

theory,

$$
\begin{bmatrix} i_p \\ i_q \end{bmatrix} = \begin{bmatrix} \sin(wt) & -\cos(wt) \\ -\cos(wt) & -\sin(wt) \end{bmatrix} \begin{bmatrix} i_\alpha \\ i_\beta \end{bmatrix}
$$
$$
= \begin{bmatrix} \bar{i}_p \\ \bar{i}_q \end{bmatrix} + \begin{bmatrix} \tilde{i}_p \\ \tilde{i}_q \end{bmatrix}
$$

(1)

In the above equations, $\sin(wt)$ and $\cos(wt)$ are standard sinusoidal signals

synchronized through phase-lock loop. $\bar{i}_p$ and $\tilde{i}_p$ represent dc and ac components of the

active current respectively. $\bar{i}_q$ and $\tilde{i}_q$ represent dc and ac components of the reactive

current respectively.

The components of fundamental currents $i_{\alpha f}$ and $i_{\beta f}$ can be achieved through $\bar{i}_p$

and $\bar{i}_q$ according to the equation,

$$
\begin{bmatrix} i_{\alpha f} \\ i_{\beta f} \end{bmatrix} = \begin{bmatrix} \sin(wt) & -\cos(wt) \\ -\cos(wt) & -\sin(wt) \end{bmatrix} \begin{bmatrix} \bar{i}_p \\ \bar{i}_q \end{bmatrix}
$$
$$
= \begin{bmatrix} \sqrt{2}I_1 \sin(wt - \Phi_1) \\ \sqrt{2}I_1 \sin(wt - \Phi_1 - \frac{T}{4}) \end{bmatrix}
$$

(2)

The whole current minus fundamental component is the harmonic component of current. Figure 3 is the APF PI control scheme.
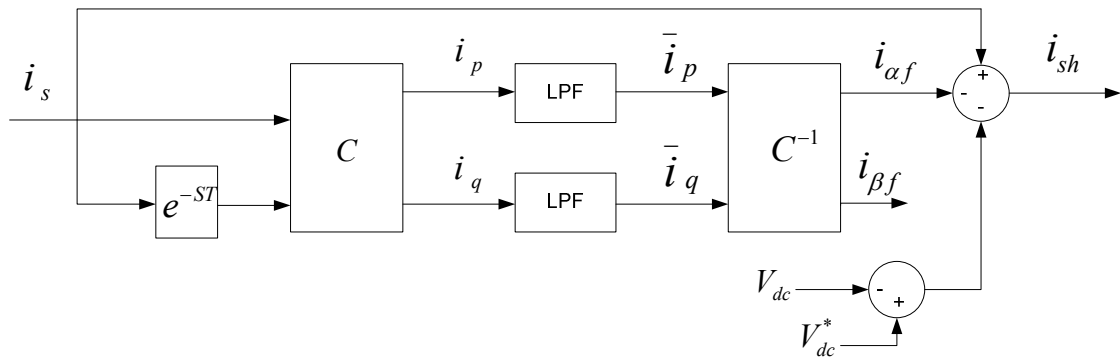
$$i_{sh} = i_\alpha - i_{\alpha f}$$

(3)

Fig. 3 Single phase APF PI control scheme

In addition, the APF part can build up and regulate the dc capacitor voltage during the UCAP recharging mode. If the active filter outputs a fundamental voltage that is in phase with the fundamental leading current of the passive filter, the active power formed by the leading current and the fundamental voltage is supplied to the dc capacitor. Therefore in the dc voltage feedback loop $i_{\alpha f}$ is the electrical quantity to be controlled.

From Figure 3, since the low-pass filter has response time, so the $\bar{i}_p$ will have some delay if the load fundamental frequency current is changed. This can affect the APF active power flow and DC-link voltage. It will be shown in the simulation results.

III. H∞ CONTROL METHOD FOR UPQC

The H∞ optimal control system is to evaluate a regular real rational controller K, which is aimed to keep the closed-loop system internally stable and to minimize the track error [8]. Typical solving methods are Riccati and LMI.

A. Standard H∞ Control Scheme

Figure 4 is the H∞ standard control system. The control model G is combination of ideal model transfer function M and known control object P. Its state space model is:

$$\begin{cases} \dot{x} = Ax + B_1 w + B_2 u \\ z = C_1 x + D_{11} w + D_{12} u \\ y = C_2 x + D_{21} w + D_{22} u \end{cases} \tag{4}$$

K is a controller to be designed; x is the state variable vector; w is the reference input set; u is control input set. z is the output of errors to be minimized; y is output of feeding to the controller K.
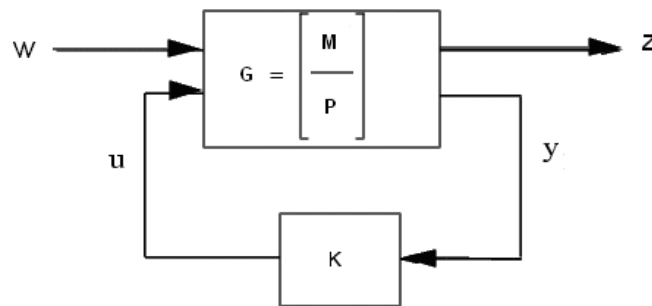

Fig. 4 Standard H∞ control scheme

The H∞ control method can be applied in UPQC's DVR and APF part for power quality waveform tracking compensation. To actualize the control of power quality waveform, the state space expression of ideal model M and the mathematical model of the controlled object P should be established.

The ideal model M in the system is an expected filter transfer function. Considering the factors of actual harmonic orders contained in the compensated load and compensation control strategy etc., M is regarded as a band-pass filter, its transfer function is

$$M(s) = \frac{b_m s^m + b_{m-1} s^{m-1} + \ldots + b_1 s + b_0}{s^n + a_{n-1} s^{n-1} + \ldots + a_1 s + a_0}; m < n \tag{5}$$

The mathematical model of the controlled object P is built up by the state equations of the power quality controller DVR and APF.

$$\begin{cases} \dot{x} = Ax + Bu \\ y = Cx \end{cases} \tag{6}$$

Having obtained M and P, according to Figure 4, the state space implementation of the general control model G for UPQC can be processed further. The H∞ optimal controller K(s) is realized by using the relative functions in MATLAB.

B. DVR Part Control

The DVR single-phase equivalent circuit is represented in Figure 5, which is serial connected with the distribution system. The mathematical model of the controlled object P for DVR part can be established with its equivalent circuit.
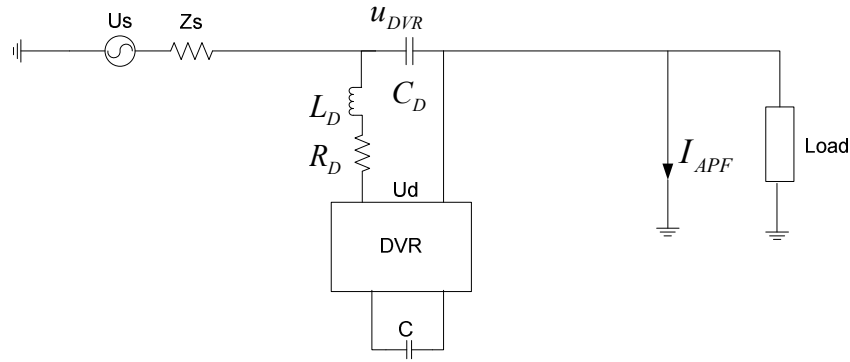
Fig. 5 Equivalent circuit of UPQC DVR part

The DVR equivalent circuit topology is mainly composed of the voltage inverter part and passive filter part. In Figure 5, U_D is the output voltage of the inverter, it is equivalent to an alternating controlled voltage source. R_D is the equivalent resistance relating to the switch loss of the inverter and the active power loss of the passive filter part and serial transformer, L_D is the summation of the filtering inductance and transformer leakage inductance , C_D is the filter capacitance.

The capacitance voltage u_{DVR} of the filtering segment is the compensation voltage. In the state space expression of DVR, the state variable $x = \begin{bmatrix} x_1 \\ x_2 \end{bmatrix} = \begin{bmatrix} u_{DVR} \\ \dfrac{du_{DVR}}{dt} \end{bmatrix}$, the control variable $u = \begin{bmatrix} u_D - R_D i_l - L_D \dfrac{di_l}{dt} \end{bmatrix}$, the output variable $y = [x_1] = [u_{DVR}]$. DVR state model parameters are:

$$A = \begin{bmatrix} 0 & 1 \\ -\dfrac{1}{L_D C_D} & -\dfrac{R_D}{L_D} \end{bmatrix}, B = \begin{bmatrix} 0 \\ \dfrac{1}{L_D C_D} \end{bmatrix}, C = \begin{bmatrix} 1 & 0 \end{bmatrix} \qquad (7)$$

In this way the controlled object P for DVR part is established. The ultimate output of DVR part is the controlled voltage source.

C. APF Part Control

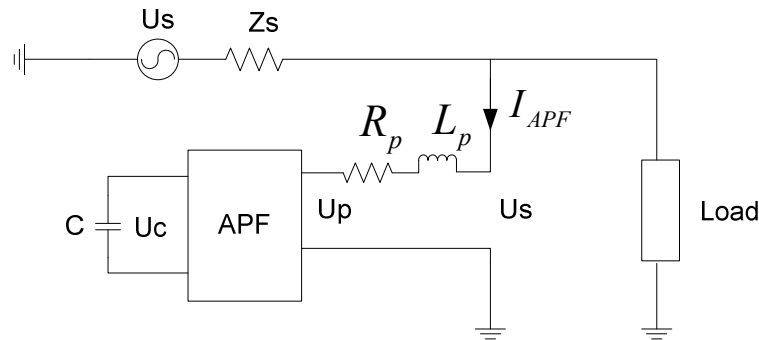The equivalent circuit of UPQC APF part is represented in Figure 6.

Fig. 6 Equivalent circuit of UPQC APF part

In Figure 6, U_C is the voltage of the capacitance C in the DC-link of APF. The inverter output voltage of APF part is U_p, it is equivalent as an alternating controlled voltage source. The resistance R_p represents the switching loss of inverter and the active loss of the filter and shunt transformer. L_p is the summation of the filtering inductance and transformer leakage inductance. The filtering inductance current is the compensating current I_{APF}. In the state space expression of APF, the state variable $x = [I_{APF}]$, the

control variable $u = \begin{bmatrix} u_p - u_s \end{bmatrix}$, the output variable y is I_{APF}. The parameters for APF state model are:

$$A = \begin{bmatrix} -\dfrac{R_p}{L_p} \end{bmatrix}, B = \begin{bmatrix} \dfrac{1}{L_p} \end{bmatrix}, C = \begin{bmatrix} 1 \end{bmatrix} \tag{8}$$

In this way the controlled object P for APF part is established. The ultimate output of APF part is a controlled current source.

At first the H∞ optimization controller K1(s) of fundamental frequency component is calculated, so are the optimization controllers K3(s), K5(s), K7(s), which compensate 3rd, 5th, 7th harmonic, etc. Then the overall H∞ optimization controller K(s) of dynamic tracking waveform can be obtained by assembling these controller modules.

Next with the actual UPQC parameters the optimal controller K is calculated by using the above H∞ method in MTLAB. The tracking simulation experiments for 3rd, 5th, and 7th harmonic components will be performed to validate the correctness of this method. Then the controller K is applied in UPQC simulation environment, and a three-phase rectifier load is applied at the load side for practical application.

IV. H∞ CONTROLLER REALIZATION IN MATLAB

With the state space implementation, the H∞ optimization controller K can be achieved in MATLAB [9]. First the system state model is processed, which is partitioned to a TITO (two-input-two-output) system. Then an optimal H∞ controller for a partitioned system matrix is calculated. The DVR and APF state model can be built up in MATLAB, as in Figure 7, with the H∞ control feedback.
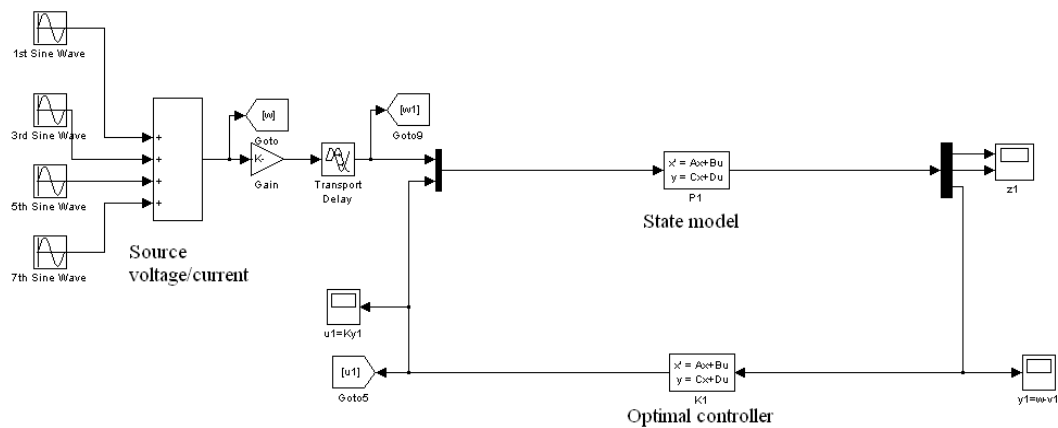

Fig. 7 DVR and APF state models in MATLAB

For the DVR part, given the source side voltage 1st order magnitude is 2 p.u., 3rd, 5th, 7th harmonic magnitude is 1 p.u.. In MATLAB simulink the DVR output that tracking the system voltage is as in Figure 8. The result shows that after about 2 power cycles, the DVR can track the system voltage quite well with very small error by using H∞ controller.

The MALAB simulink topology of APF is similar with DVR. With the APF state model its H∞ controller K can be calculated. The APF only need to track the harmonic components of load current. The result is shown in Figure 9. Like in the DVR case, the controller also need about 2 power cycles to tracking the harmonics. In the next section we will show that this will affect H∞ application.

After getting the optimal controller K in MATLAB, it can be applied in UPQC simulation environment, and a three-phase rectifier load is applied at the load side for practical application.
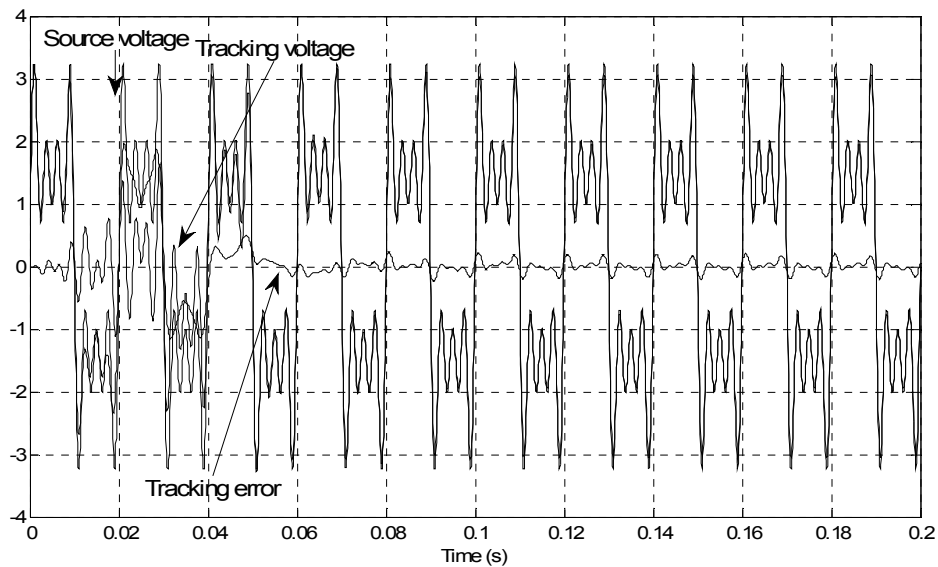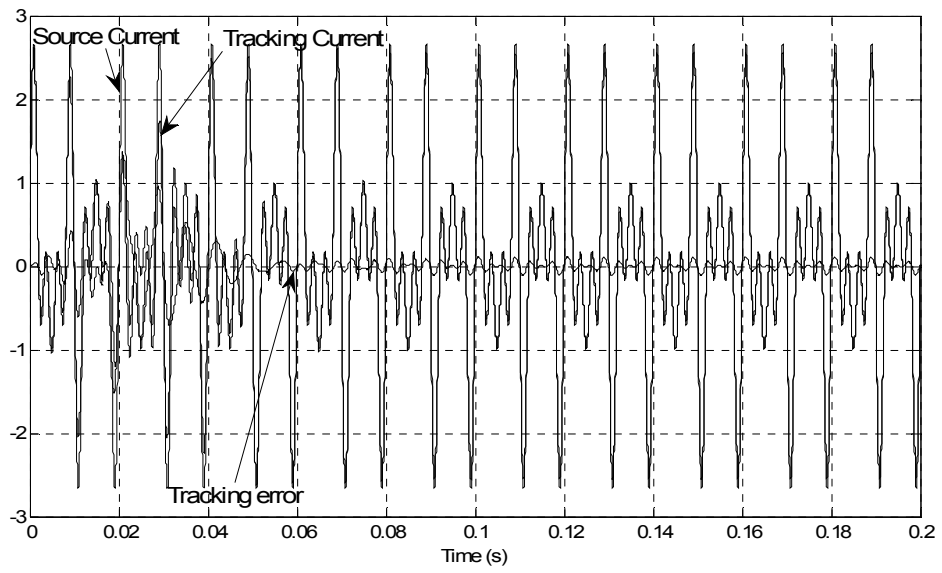
Fig. 8 DVR state model tracking result

Fig. 9 APF state model tracking result

V. UPQC SIMULATION RESULTS

Based on the PI and H∞ method mentioned above, the UPQC simulation environment is built in EMTDC/PSCAD, as in Figure 10. The UPQC topology has the DC-link which is connected with an energy storage system based on UCAP. DVR and APF part share this same DC-link. The two control methods are applied to the UPQC simulation. The performance is compared in different transit states.
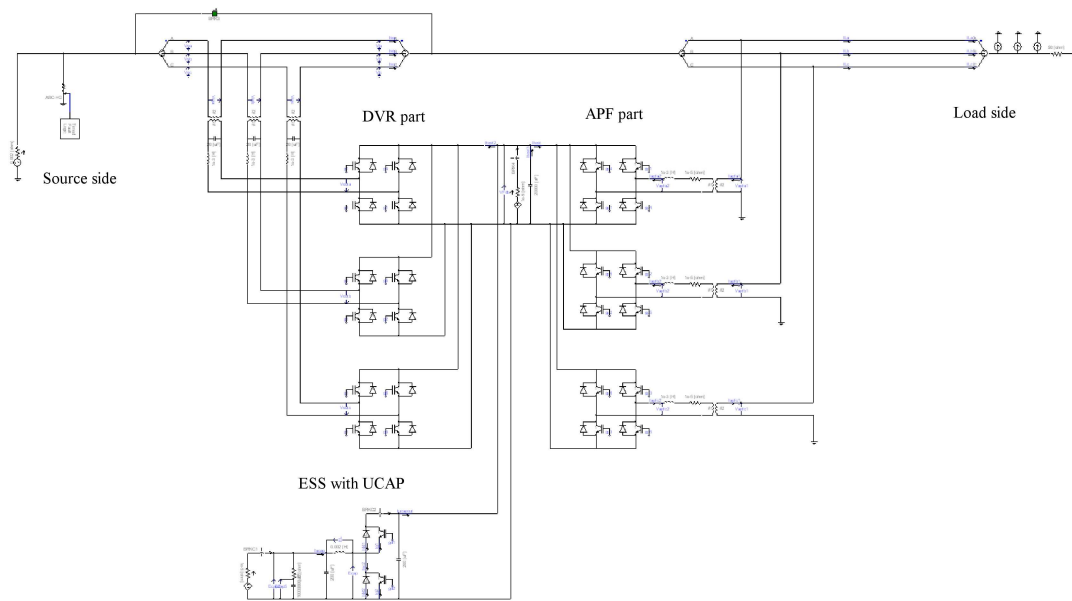

Fig. 10 UPQC simulation topology in PSCAD

A. DVR Part Result

Since the DVR part is mainly focus on the fundamental frequency voltage, the H∞ method is used to track fundamental frequency voltage. When a fault happens, the

load voltage can be restored within 2 power cycles time. The simulation result is as Figure 11. This delay is not happened in the DVR PI control method. Therefore for better performance the UPQC always use PI method for its DVR part.
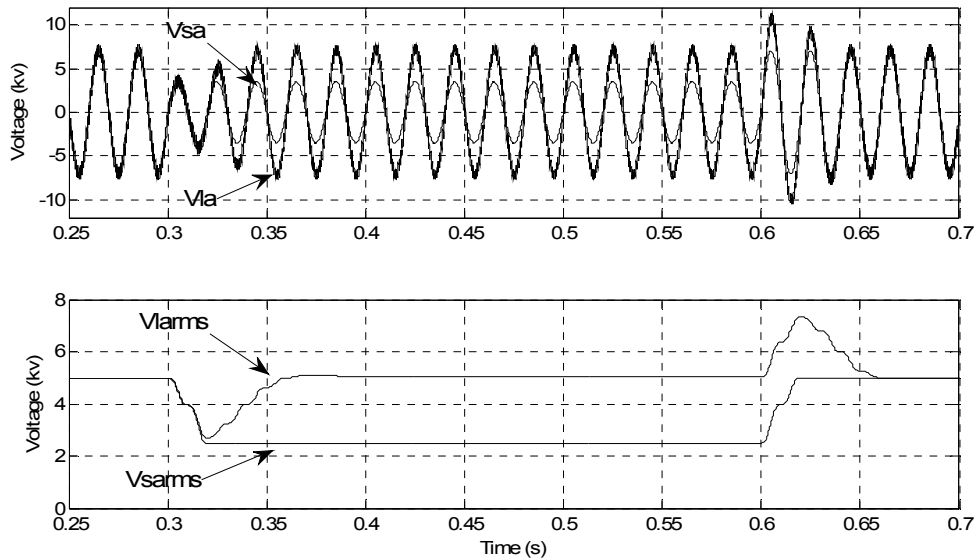

Fig. 11 DVR performance with H∞ method

B. APF Part Results Comparison

To test the APF control scheme, a current harmonic load combined by 3rd, 5th, 7th order is shunt connected with a regular R-L load. By changing the regular and harmonic load rating, the PI and H∞ controller schemes' performance is compared. In the simulation the bus voltage level is 5kv, DC-link voltage is 3.8kv, and each of the three harmonics magnitude is 0.08kA. Originally the load side current THD is 30%.

If regular load rating is changed from 15Ω to 30Ω then back to 15Ω , Figure 12 is the simulation result with PI method. Since the response time of the low pass filter in the PI control scheme, the detection of the fundamental frequency current I_{pa} is delayed, so is the control current I_{α}. This causes the surge of DC-link voltage V_{dc}. It is also shown in the surge of the APF active power output P_{apf}.

If regular load rating is changed, the result is as Figure 13 with H∞ method. Changing regular load means only fundamental frequency current is changed. H∞ method only tracks the harmonics part so there has no active power exchange between UPQC and system. V_{dc} keeps stable and Source current THD I_{sathd} response is fast.

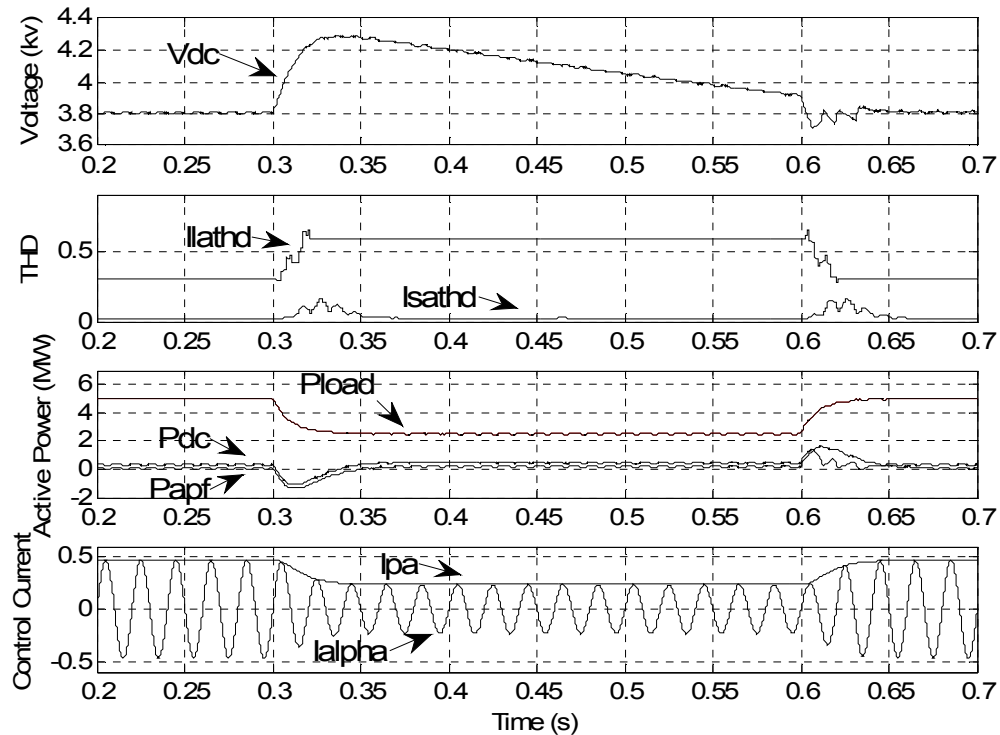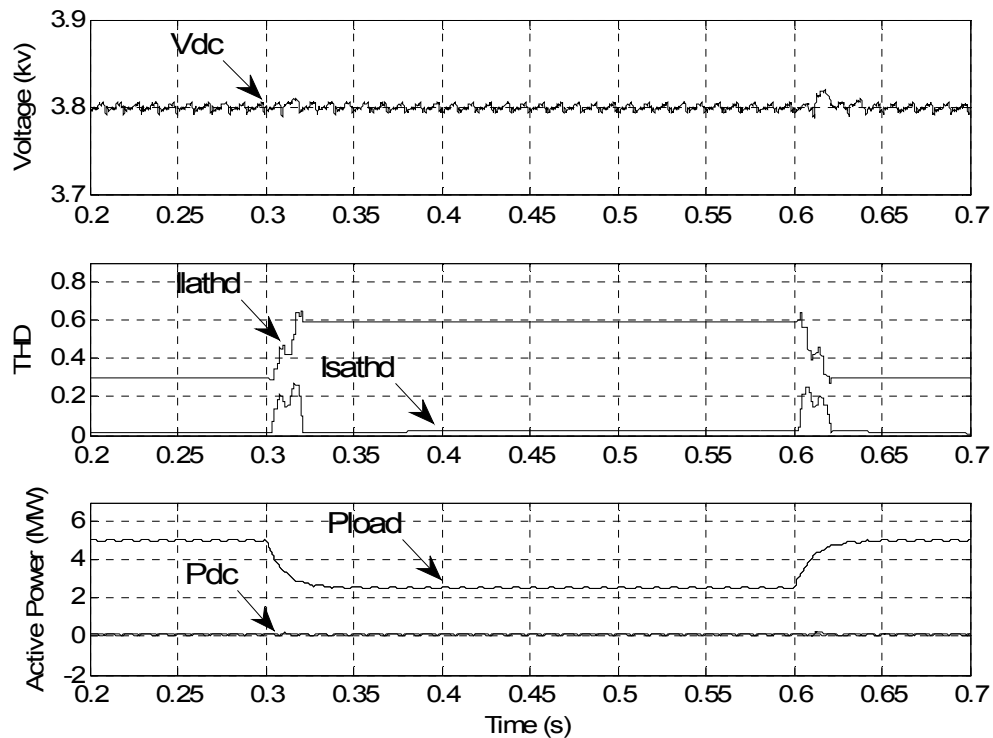Fig. 12 APF performance with PI method when regular load is changing

Fig. 13 APF performance with H∞ method when regular load is changing

If the harmonic load rating is changed from 0.08kA to 0.15kA then to 0.08kA, the result is as Figure 14 with PI method. If only harmonic is changed, fundamental tracking is not affected, as in I_{pa} and I_{α}. There has no active power exchange and V_{dc} has no surge.

If the harmonic load rating is changed, the simulation result is as Figure 15 with H∞ method. The detecting of harmonic makes the controller has delay time, the reaction time is about 2 power cycles. It is shown in I_{sathd} curve. Since the harmonics doesn't

affect the active power, there has no active power exchange and DC-link voltage V_{dc} keeps stable.

In summary, for the PI control method, since the response time of the low pass filter the fundamental frequency current tracking has delay when regular load is changed. This causes the active power exchange between UPQC and system, and the surge of DC-link voltage V_{dc}. But if only harmonics current is changed, PI method works fine. There has no power exchange and V_{dc} keeps stable.

For the H∞ method, the detection of harmonic components has delay. When the harmonic load is changed, it takes about 2 power cycles to track the harmonics. This is shown in the I_{sathd} curve. But if only regular load is changed, the H∞ method works fine. There has no active power exchange and V_{dc} keeps stable. The advantages and disadvantages of the two control methods are summarized in Table 1.

Table 1. Comparison between PI and H∞ method in APF

	PI	H∞
Change regular load	Active power exchange; V_{dc} has surge.	V_{dc} has no surge
Change harmonic load	Fast response for harmonic compensation	Harmonic compensation has delay, shown in I_{sathd}

So in the practical application if the regular load is changed, H∞ method has better performance. If harmonic load is changed, PI method is better.
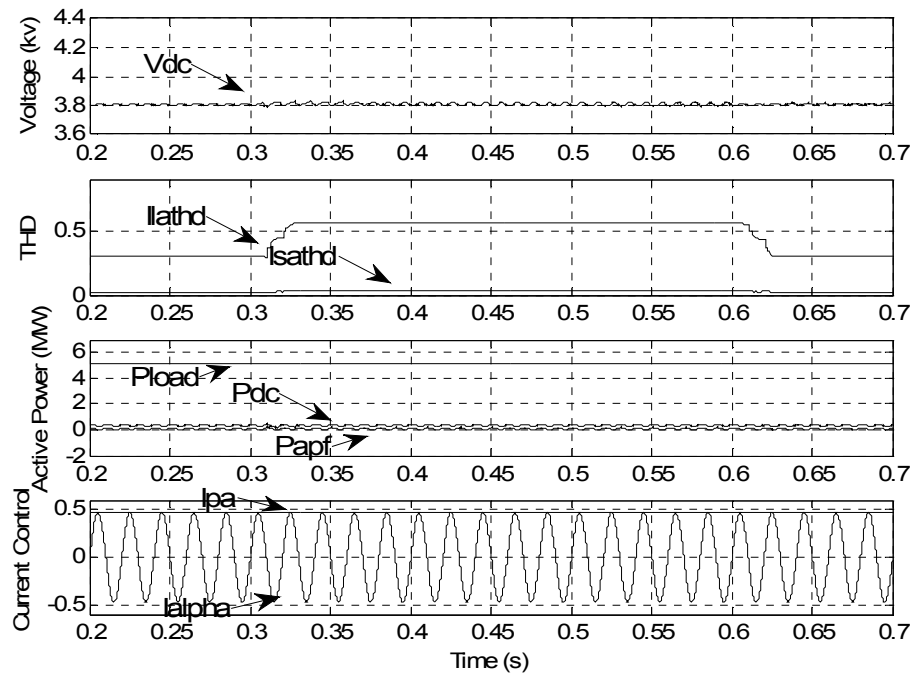
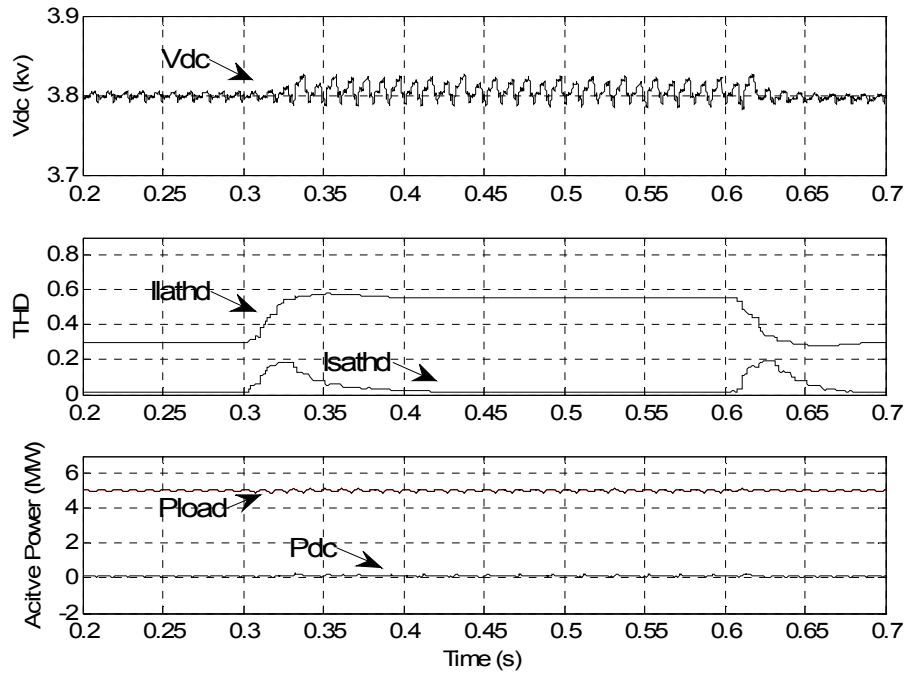Fig. 14 APF performance with PI method when harmonic load is changing

Fig. 15 APF performance with H∞ method when harmonic load is changing

C. H∞ Method With DC Voltage Control Function

Like in the PI method, H∞ method in APF can also add DC-link voltage control into the control scheme to recharge the UCAP in the UPQC topology.

The result of charging UCAP is shown in Figure 16. UCAP internal model voltage is charged from 1.2kv to 1.5kv, beginning from 0.3s. The charging current is limited for the active power flow limit in APF part.
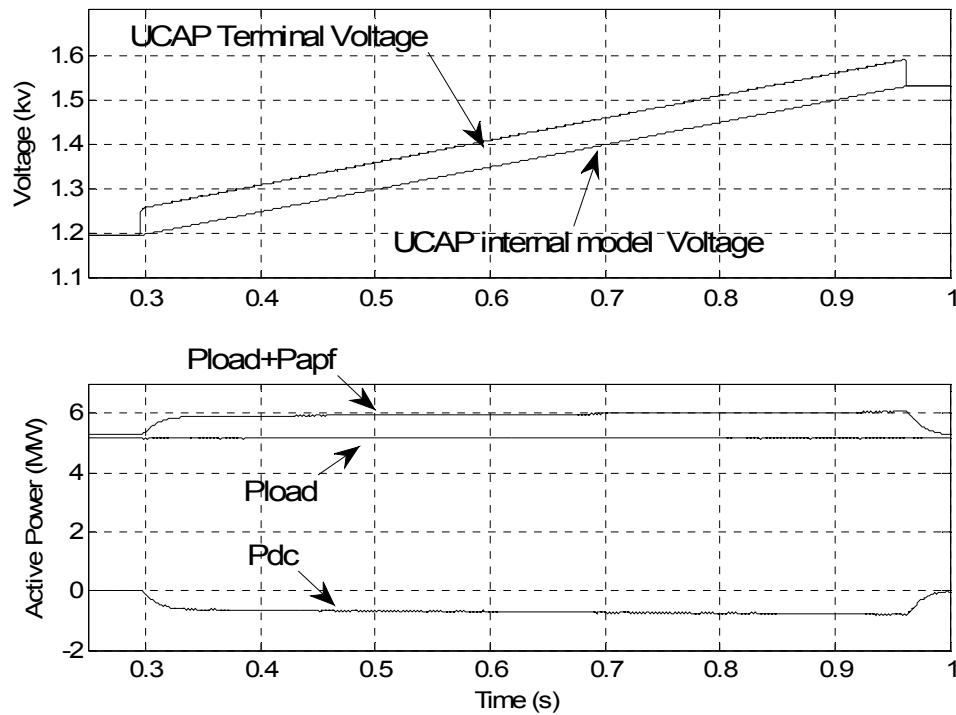

Fig. 16 UCAP in ESS recharging using H∞ method

D. Results Comparison With 3-phase Rectifier Load

For practical application a 3-phase rectifier load is shunt connected with the regular load, shown in Figure 17. In the simulation the bus voltage level is 5kv, DC-link voltage is 3kv. The 3-phase rectifier load contains 30% THD with 6k +/-1 order harmonics. The 3-phase rectifier DC-link resister load is 50Ω . The regular load is 30Ω .

The overall load current THD is about 14.9%. Since most of the harmonic are 5th, 7th, 11th, 13th order harmonics, in the simulation the H∞ controller is combined by the four order modules.
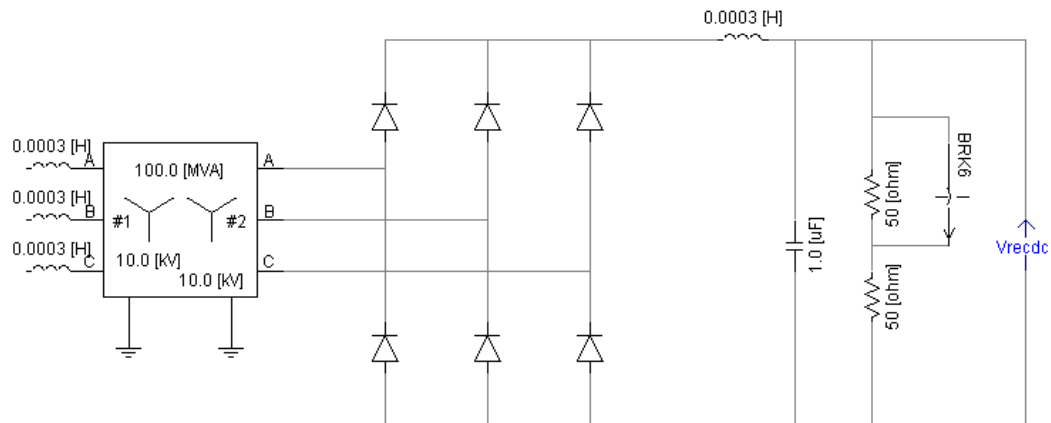

Fig. 17 3-phase rectifier load

If the regular load rating is changed from 30Ω to 80Ω then to 30Ω , the result is as Figure 18 with PI method. Since the response time of the low pass filter in the PI control scheme, the detection of the fundamental frequency current I_{pa} is delayed, so is

the control current I_α. This causes the surge of DC-link voltage V_{dc}. It is also shown in the surge of the APF active power output P_{apf}.

If regular load rating is changed, the result is as Figure 19 with H∞ method. Changing regular load means only fundamental frequency current is changed. H∞ method only tracks the harmonics part so there has no active power exchange between UPQC and system. V_{dc} keeps stable and Source current THD I_{sathd} response is fast. The four harmonic compensation components drop I_{sathd} to 2%.

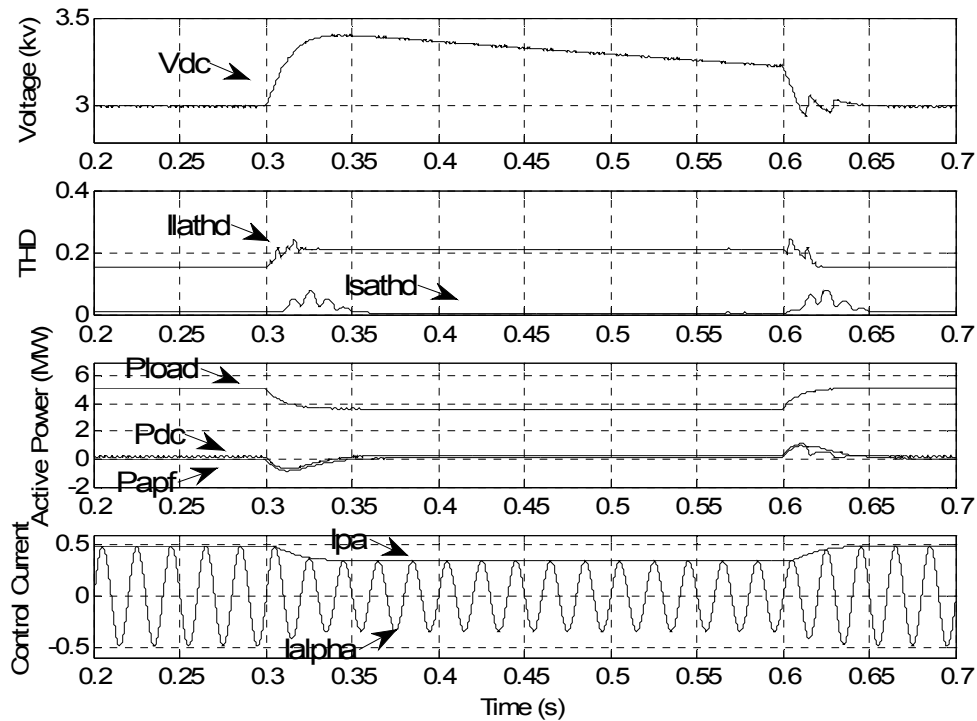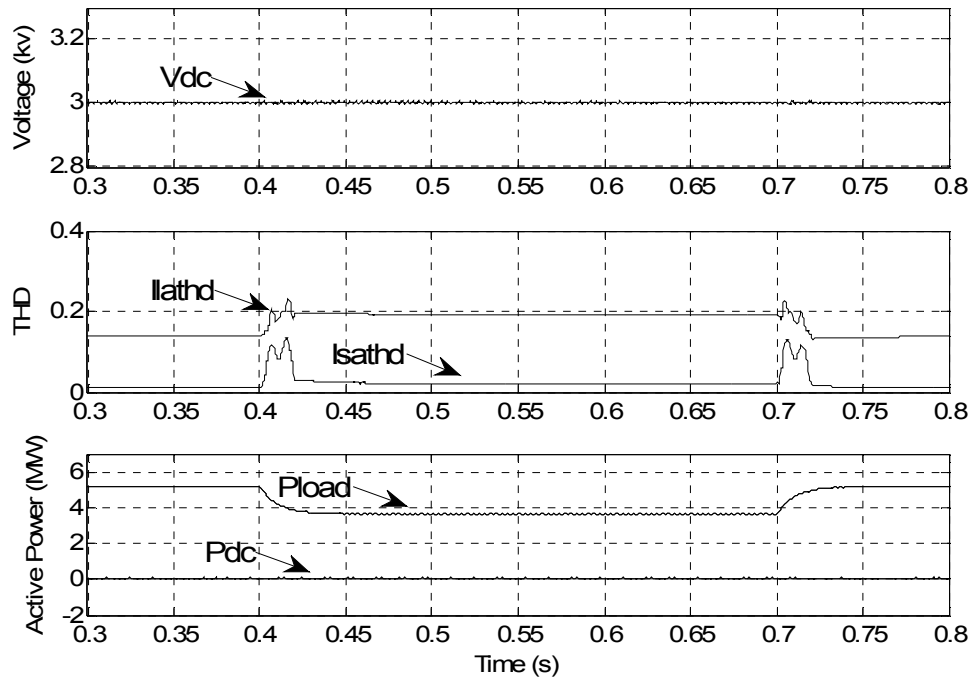Fig. 18 APF performance with PI method when regular load is changing

Fig. 19 APF performance with H∞ method when regular load is changing

If the rectifier DC load is changed from 50Ω to 100Ω then to 50Ω, the result is as Figure 20 with PI method. Since changing the rectifier DC load also affect the fundamental frequency current, the PI method still make the UPQC DC-link voltage V_{dc} surge. The curve I_{pa} and I_{α} shoe the control current and P_{apf} show the active power flow.

If the rectifier DC load is changed the result is as Figure 21 with H∞ method. Since harmonic rating is changed, so the H-infinity method has some delay, shown in I_{sathd} curve. But there has no active power exchange and the DC-link voltage V_{dc} keeps stable.
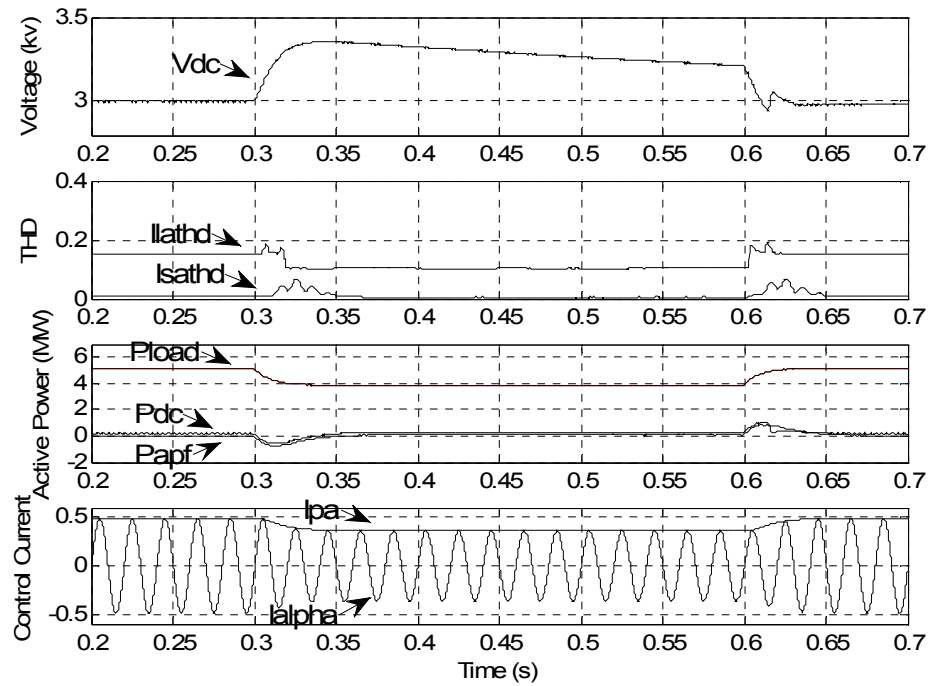
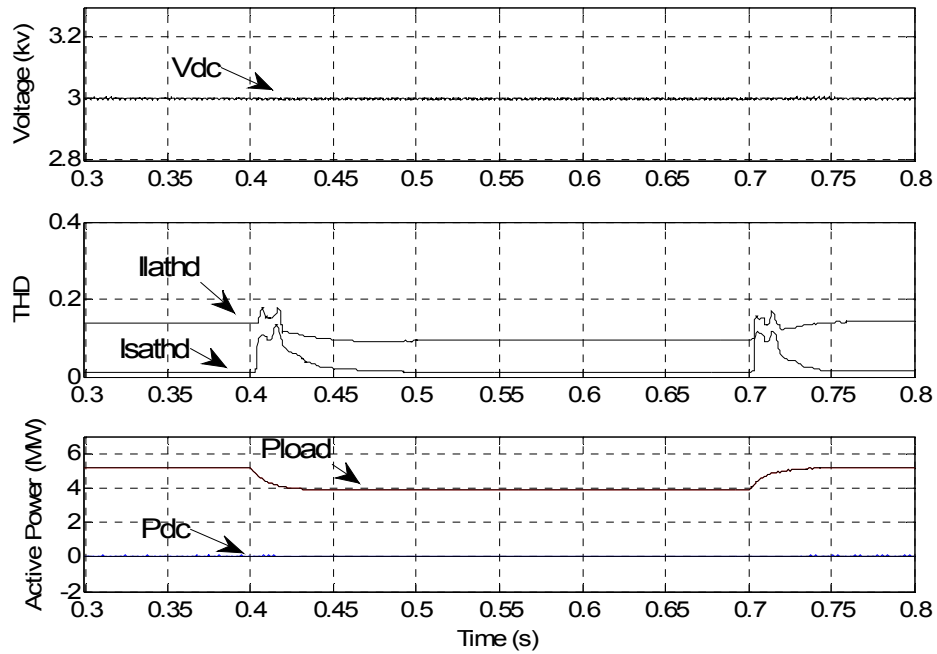Fig. 20 APF performance with PI method when harmonic load is changing

Fig. 21 APF performance with H∞ method when harmonic load is changing

VI. APPLICATION AREA OF PI AND H∞ METHOD

The UPQC is a distribution–level power quality improvement device. Since PI method is easily make V_{dc} surge, if the system voltage/power rating is relatively high, V_{dc} surge will dramatically impact the UPQC performance, including switching losses, system components (IGBT, capacitor, inductor, transformer) rating, and system efficiency. H∞ method always keeps V_{dc} stable. So in high voltage/power rating system, like a small residential area, office building, etc, H∞ method is better.

In a relatively low voltage/power rating system, V_{dc} surge caused by PI method is very limited and there has a low demand for system components rating. V_{dc} surge is not a big problem. But generally this kind of system, like arc furnace, machine tool, etc, demands fast response of harmonic elimination, and the harmonic load is often changed from time to time. So PI method is better for its fast harmonic response in this kind of system. The two methods application area is summarized in Table 2.

Table 2. Application area of PI and H∞ method

	Application area
PI method	Low voltage/power rating system; Load harmonic condition changes frequently. Like arc furnace, machine tool, etc.
H∞ method	Higher voltage/power rating system; Load harmonic condition keeps stable. Like a resident area, office building.

VII. CONCLUSIONS

Conventionally the PI control method is applied in UPQC control scheme, including DVR and APF part. Recently the H∞ control method is applied in the Power Quality area. This paper shows the difference of the two control schemes, and performance is compared under different conditions. The simulation result shows that the two methods have their own advantages and disadvantages. If the regular load is changed frequently, H∞ method has better performance. If harmonic load is changed frequently, PI method is better. In the practical application the control method can be chosen by considering the different application area.

VIII. REFERENCES

1. A. Ghosh, G. Ledwich, "A Unified Power Quality Conditioner (UPQC) for Simultaneous Voltage and Current Compensation," Electric Power Systems Research, vol. 59(1), Page(s): 55-63, 2001.

2. V. Khadkikar, A. Chandra, "A new control philosophy for a unified power quality conditioner (UPQC) to coordinate load-reactive power demand between shunt and series inverters," IEEE Trans. on Power Delivery, vol. 23(4), October 2008.

3. D. Dorr, M. Hughes, T. Gruzs, R. Jurewicz, and J. McClaine, "Interpreting recent power quality surveys to define the electrical environment," IEEE Trans. on Industry Applications, vol. 33(6), November/December 1997.

4. Li Peng, Li Heming, Wei Bing, Yang Yihan, "A Novel Control Method of Power Quality Waveform Tracking Compensation Based on H-Infinity Model Matching Technology," 2004 International Conference on Power System Technology, Singapore, 21-24 November 2004.

5. A. Kara, P. Dahler, D. Amhof, H. Gruning, "Power supply quality improvement with a dynamic voltage restorer (DVR)," Applied Power Electronics Conference and Exposition, vol. 2, Page(s):986 - 993, 1998.

6. H. Fujita, H. Akagi, "A practical approach to harmonic compensation in power systems-series connection of passive and active filters," IEEE Transactions on Industry Applications, vol. 27(6), 1991.

7. J. Liu, J. Yang, Z. Wang, "A new approach for single-phase harmonic current detecting and its application in a hybrid active power filter," Industrial Electronics Society, vol. 2(29), 1999.

8. D. W. Gu, P. Hr. Petkov and M. M. Konstantinov, "Robust Control Design with MATLAB," ISBN-10: 1852339837, Chapter 4.3, 2005.

9. "MATLAB Robust Control Toolbox, User's Guide," Version 3, the Math Works, Inc., 2005.

VITA

Xiaomeng Li was born in China in January 3, 1980. After six years in Xinmi City High School, he began his study in Tsinghua University, Beijing, China in 1997. He received his BS and MS degree in Electrical Engineering in 2001 and 2004. In 2004, he began pursuing his PhD in the Electrical and Computer Engineering department at Missouri University of Science and Technology. He served as a graduate research assistant. His research interests were Power Quality, distribution power device and Energy Storage System application in distribution power system. He graduated in May, 2010 from Missouri University of Science and Technology with his PhD.